EXPLORATION INTO THE CELLULAR EFFECTS OF AZIRIDINOMITOSENES

by

Christopher M. Mallory

A thesis

submitted in partial fulfillment

of the requirements for the degree of

Master of Science in Chemistry

Boise State University

August 2014

BOISE STATE UNIVERSITY GRADUATE COLLEGE

DEFENSE COMMITTEE AND FINAL READING APPROVALS

of the thesis submitted by

Christopher M. Mallory

Thesis Title: Exploration into the Cellular Effects of Aziridinomitosenes

Date of Final Oral Examination: 03 July 2014

The following individuals read and discussed the thesis submitted by student Christopher M. Mallory, and they evaluated his presentation and response to questions during the final oral examination. They found that the student passed the final oral examination.

Don L. Warner, Ph.D.	Chair, Supervisory Committee
Ken Cornell, Ph.D.	Member, Supervisory Committee
Kristen Mitchell, Ph.D.	Member, Supervisory Committee

The final reading approval of the thesis was granted by Don L. Warner, Ph.D., Chair of the Supervisory Committee. The thesis was approved for the Graduate College by John R. Pelton, Ph.D., Dean of the Graduate College.

DEDICATION

I would like to dedicate this work to all my loved ones that were there for me day in and day out. To all of you that gave me hope, support, and a kind ear, I am forever indebted.

ACKNOWLEDGEMENTS

I would like to acknowledge Dr. Don L. Warner and Dr. Ken A. Cornell for the opportunity to work on this research project, in their laboratories, and the constant lessons in science and life they kindly provided. I would also like to thank Dr. Denise Wingett, Dr. Cheryl Jorcyk, and Dr. Kristen Mitchell for providing the cell lines in this work; this research would not have been possible without their generous contributions. Thank you to Dr. Julie Oxford for allowing me to continually use her fluorescent microscope. Further, I would like to thank the members of my committee, Dr. Ken Cornell and Dr. Kristen Mitchell, for their time, contributions, and support of my work. A special thank you goes out to my lab mates and their constant efforts to synthesize the aziridinomitosenes used in these studies. Lastly, thank you to the Boise State Department of Chemistry and Biochemistry for this opportunity and support along the way.

I would also like to acknowledge all of the funding sources that supported this research; these grants awards include NIH R15 (2R15CA113464-02, Warner, PI), and the Idaho Global Entrepreneurial Mission University Infrastructure Grant program.

ABSTRACT

Aziridinomitosenes (AZMs) are organic compounds structurally related to the mitomycins, a class of anti-tumor agents and antibiotics. The cytotoxicity of the mitomycins is correlated to their ability to covalently link complimentary strands of DNA, forming DNA interstrand cross-links (ICLs). Currently, there has been limited investigation into the biological activity of AZMs, likely due to difficulties in their synthesis. Our lab has synthesized and evaluated the cellular effects of two AZMs, (1S, 2S)-6-desmethyl(methylaziridino)mitosene (H/H-AZM) and (1S, 2S)-6-methyl(methylaziridino)mitosene (Me/H-AZM**)**. We hypothesize that AZMs exhibit their cytotoxicity and cellular effects following a similar pathway to that of mitomycin C (MC), including the ability to form ICLs and modify DNA in cellular systems. To test this hypothesis, we evaluated the cytotoxicity of our AZMs compared to MC in six cancer cell lines. Previously, MC has also been shown to lead to the production of reactive oxygen species (ROS), activation of caspase enzymes, changes in mitochondrial membrane potential, and nuclear swelling. As such, we probed for these effects in Jurkat and HeLa cancer cells upon AZM and MC treatment. Our studies reveal that the Me/H-AZM has increased cytotoxicity compared to MC, while H/H-AZM was only more potent than MC in the T47D breast cancer cell line. Both AZMs were more effective at increasing the levels of oxidative stress over MC. Changes to the mitochondrial membrane potential were equivalent or greater than MC in treatments with both AZMs. Additionally, all three compounds were found to increase caspase-3 activation, with MC

leading to the greatest amount of activity in the Jurkat cell line. Only MC treatment significantly increased caspase-3 activation in HeLa cells. Both AZM and MC treatment stimulated nuclear swelling. Finally, the DNA modifying-abilities of AZMs were investigated with the use of a Hoechst 33342 DNA cross-linking assay and a modified alkaline COMET assay. Of the three compounds tested, these studies found that Me/H-AZM lead to highest formation of DNA-DNA cross-links and modification to cellular DNA. H/H-AZM treatment was found to produce a larger amount of cross-links and DNA modification in Jurkat cells than MC, but showed similar results to MC in HeLa cells. Overall, AZMs were found to possess similarities to MC in their cellular effects in Jurkat and HeLa cells, with the ability to alkylate DNA in cell systems.

TABLE OF CONTENTS

LIST OF TABLES

LIST OF FIGURES

LIST OF ABBREVIATIONS

ANOVA	Analysis of Variance
AZM	Aziridinomitosene
BSA	Bovine Serum Albumin
C	Cytosine
CCCP	Carbonyl Cyanide 3-chlorophenylhydrazone
COMET	Single Cell Gel Electrophoresis
DAM	2,7-diaminomitosene
DAPI	4’,6-diamidino-2-phenylindole
DCFDA	2’,7’-dichlorodihydrofluorescein Diacetate
DG	Deoxyguanosine
DI	Deionized
DMC	Decarbamoyl Mitomycin C
DMEM	Dulbecco’s Modified Eagle’s Medium
DMSO	Dimethyl Sulfoxide
DNA	Deoxyribonucleic Acid
DPC	DNA-protein Cross-link
dsDNA	Double Stranded Deoxyribonucleic Acid

ESR	Electron Spin Resonance
FAD	Flavin Adenine Dinucleotide
FBS	Fetal Bovine Serum
G	Guanine
H/H-AZM	(1S, 2S)-6-desmethyl(methylaziridino)mitosene
H_2O_2	Hydrogen Peroxide
ICL	Interstrand Cross-link
IMDM	Iscove's Modified Dulbecco's Medium
JC-1	5,5′,6,6′-tetrachloro-1,1′,3,3′-tetraethylbenzimidazolocarbocyanine iodide
KRB	Kreb's Ringer Bicarbonate
MA	Mitomycin A
MA-AZM	Mitomycin A Aziridinomitosene
MB	Mitomycin B
MC	Mitomycin C
MC-AZM	Mitomycin C Aziridinomitosene
MCRA	Mitomycin C Resistance Associated
Me/H-AZM	(1S, 2S)-6-methyl(methylaziridino)mitosene
MED	Minimum Effective Dose
$NaBH_4$	Sodium Borohydride

NAC	N-acetyl-L-cysteine
NADH	Nicotinamide Adenine Dinucleotide
NADPH	Nicotinamide Adenine Dinucleotide Phosphate
NMA	N-methyl Mitomycin A
NMA-AZM	N-methyl Mitomycin A Aziridinomitosene
PBS	Phosphate Buffered Saline
POR-AZM	Porfiromycin Aziridinomitosene
RPMI	Roswell Park Memorial Institute
ROS	Reactive Oxygen Species
ssDNA	Single Stranded Deoxyribonucleic Acid
TE	Tris-EDTA

CHAPTER ONE: AZIRIDINOMITOSENES: A BRIEF HISTORY AND POTENTIAL AS ANTI-TUMOR CHEMOTHERAPEUTICS

The mitomycins are a group of potent anti-tumor antibiotics originally isolated in 1956 by Japanese researchers from the soil bacteria *Streptomyces caespitosus*.[1] The search for new anti-tumor agents led the initial discovery of mitomycin A (MA) and mitomycin B (MB); this was soon followed by the isolation of the clinically relevant, mitomycin C (MC) from the same bacterial strain (Figure 1.1).[1-3] Four years later, an N-methylated version of MC, porfiromycin, was isolated from fermentation broths of *Streptomyces ardus* in 1960.[4]

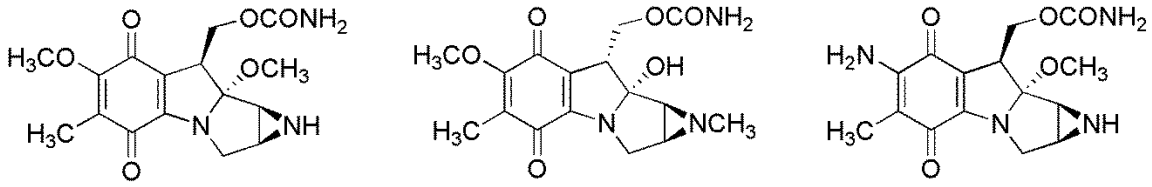

Mitomycin A **Mitomycin B** **Mitomycin C**

Figure 1.1 Structural representations of mitomycin A, B, and C.

Several detailed reviews have been published that discuss the reactivity and biochemistry of mitomycins and MC analogs.[5-11] In addition, reviews have been published outlining several approaches to the complete synthesis of mitomycins and mitomycin derivatives, "mitomycinoids".[6,12] This review is unique in the fact that it will attempt to focus primarily on aziridinomitosenes (AZMs) and their biological activity. To put this into perspective, an initial discussion regarding the structural skeletons of the

mitomycins and AZMs will be presented. From here, the isolation and initial biological activities of MC will be lightly reviewed, followed by a brief overview of the clinical utilization. A general discussion of MC affiliated DNA alkylation, oxidative stress, and anaerobic preference will conclude the discussion of MC. An overview into work with AZMs will then ensue, focusing on biological activity studies, DNA alkylation properties, and analogs with biological investigations. To finish, a brief outline to the potential benefits and drawbacks foreseen in AZM biological activity and development will be given.

Overview of Mitomycin and Aziridinomitosene Structural Skeleton

In 1962, Webb and coworkers resolved the structures of MA, MB, MC, and porfiromycin.[13,14] Confirmation of the chemically devised structure of MA was achieved through X-ray crystallography the same year.[15] These mitomycins were found to contain a tetracyclic core comprised of a fused pyrrolo[1,2-a]indole ring system, an aziridine, and carbamate functional group.[10-15] Since the initial discoveries of MA, MB, MC, and porfiromycin, numerous other mitomycin analogues have been isolated or synthesized, each containing the same core structural backbone.[10-12] The mitomycins have thus been grouped into three primary classes (A-type, B-type, and G-type) based on the substituents extending from the tetracyclic core (Figure 1.2).[6,10,12]

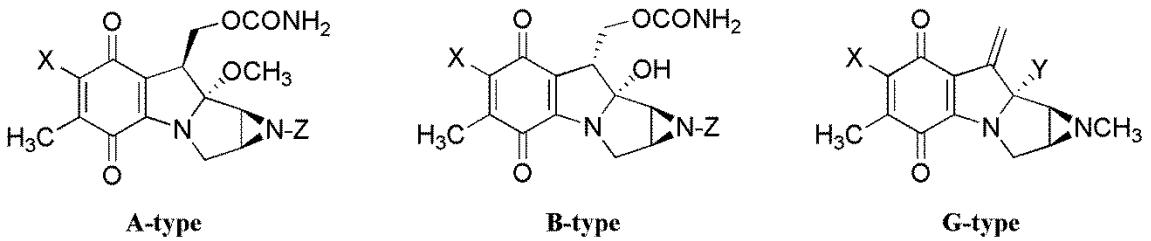

A-type **B-type** **G-type**

Figure 1.2 Structures of A-type, B-type, and G-type mitomycins.[6,12]

In 1963, Iyer and Szybalski found that MC was capable of covalently linking complimentary strands of DNA, forming a DNA interstrand cross-link (ICL). Iyer and Szybalski proposed that a reductive activation cascade of mitomycins resulting in DNA alkylation, which included the formation of a reduced aziridinomitosene (leucoaziridinomitosene) as a reactive intermediate was proposed (Figure 1.3).[17-19] Later work presented discussed that cross-linking efficiency of AZMs increased in the presence of reducing agents, supporting the assertion that the reduced AZM is the most active form of mitomycins.[18]

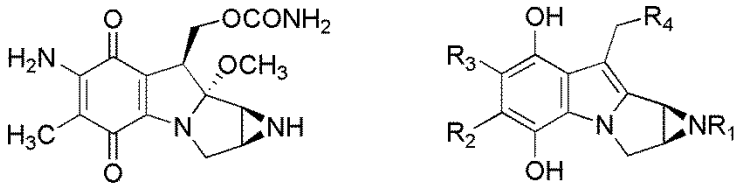

Mitomycin C **Leucoaziridinomitosene**

Figure 1.3 Structures of MC and leucoaziridinomitosene (reduced AZM).[19]

The first AZMs were characterized as degradation products of their parent mitomycins in the mid-1960s (Figure 1.4).[21] AZM synthesis was accomplished through the conversion of N-methylmitomycin A (NMA) and mitomycin B (MB) to their corresponding AZMs NMA-AZM and MB-AZM, respectively. This was accomplished via catalytic hydrogenation in N,N-dimethylformamide (DMF) at atmospheric pressure, followed by reoxidation at reduced pressure, trituration, and recrystallization.[21]

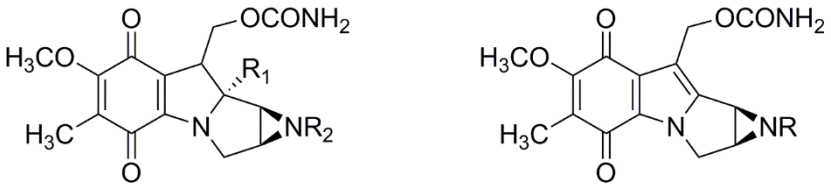

NMA $R_1 = OCH_3$, $R_2 = CH_3$ **NMA-AZM** $R = CH_3$

MB $R_1 = OH$, $R_2 = H$ **MB-AZM** $R = H$

Figure 1.4 Structural representations of N-methyl mitomycin A (NMA) and mitomycin B (MB) with their corresponding aziridinomitosenes.[21]

Structurally, mitomycins and AZMs share the same core backbone, including the presence of a tetracyclic core arranged in a 6-5-5-3 motif, with the six and three membered rings presenting as a quinone and aziridine moiety, respectively.[16] The key difference in designation as a mitosane (core of mitomycins) versus an aziridinomitosene occurs between C9 and C9a where mitosanes have a single bond, and AZMs maintain a double bond (Figure 1.5).[10]

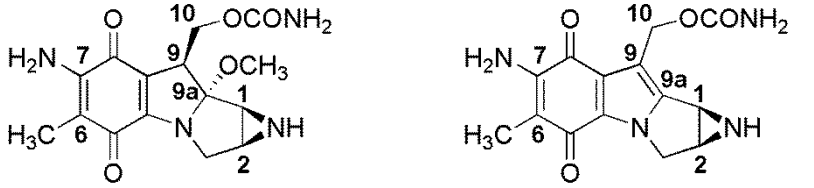

Mitomycin C **Mitomycin C Aziridinomitosene**

Figure 1.5 Structural depictions of MC and mitomycin C aziridinomitosene (MC-AZM) with partial carbon numbering scheme.

Mitomycin Isolation and Initial Studies into Biological Activity

Preliminary evaluations of purified mitomycin A, B, and C and their biological activities found these species to exhibit strong bactericidal and anti-tumor properties.[1-3] Mitomycins were found to exhibit broad spectrum antibiotic action against both gram positive and gram negative bacteria. MA was shown to be the most potent. Despite the

broad range of bacterial toxicity, effectiveness against fungi and streptomycetes was limited.[1-4]

Initial *in vivo* experiments into the anti-tumor actions of MA and MB were conducted on mice inoculated with Ehrlich ascites carcinoma. Upon confirmation of tumor growth, intraperitoneal injections of mitomycins were given at various concentrations. Three days post drug injection, tumor cells were counted and compared to the untreated group as the average days of life prolongation. This study found that mitomycin injections were able to completely abolish tumor cells, extending life up to 11 days longer than untreated mice.[1] Isolation of MC from the same bacterial broth was completed and followed with preliminary evaluations into its biological activity by Wakaki and co-workers.[3] Treatments of mice inoculated with Ehrlich ascites carcinoma showed that MC exhibited anti-tumor properties similar to MA and MB. However, drug toxicity was also demonstrated to be a problem as MC was demonstrated to cause death in mice 2-14 days post injection.[3]

Mitomycin C Clinical Use

Of the mitomycins, MC has received the most investigation and clinical use.[2,7,22] For further information regarding the clinical applications of mitomycin C, please see the reviews referenced.[22-26]

Mitomycin C has been utilized as a single agent or in combination with other chemotherapeutics. Originally MC was found to be useful in the treatment of several carcinomas, including those of the cervix, lungs, head and neck, breast, pancreas, colon, and rectum.[27] Clinical utilization of MC was linked to several side effects, including myelosuppression leading to leukopenia and thrombocytopenia. More seriously, the

possibility of renal failure that manifests even after discontinued treatment was reported.[25,27] Due to these side effects, the clinical use of MC was largely discontinued. However, MC continues to have high activity in localized treatment of bladder cancer.[23]

In addition to its use as a chemotherapeutic agent, the anti-proliferative properties of MC have found roles in other fields of medicine, including surgical and ophthalmic specialties. In ocular surgeries, MC is typically applied topically to promote the reduction of scarring and inhibition of the wound healing process, leading to prevention of haze.[26,28] The anti-proliferative effects of MC on keloid fibroblasts have led to use as an adjunct therapy in the prevention of recurring highly collagenous hypertrophic and keloid scars.[29,30] After surgical removal of the scar, application of MC to the surgical wound was demonstrated to decrease recurrence of keloid tissue.[30] Furthermore, reports of MC's potential use in otolaryngolic surgeries has been investigated in rabbits for successful use in decreasing the closure rate of maxillary sinus antrostomies.[31]

Mitomycin DNA Alkylation

In the 1960s, studies in the mitomycins biological activity revealed the formation of ICLs, with increased ICL formation occurring in species possessing greater G-C bases in their DNA.[17-19] Mitomycins were found to further inhibit DNA synthesis through additional DNA alkylating events, including mono-alkylation and intrastrand cross-linking.[32] Nine different MC-DNA adducts have been isolated and characterized from MC treated cancer cells (Figure 1.6). The isolated adducts include six different mono-alkylation and three bis-alkylated species, resulting from MC or its major cellular metabolite, 2,7-diaminomitosene (DAM).[7,11,32-38]

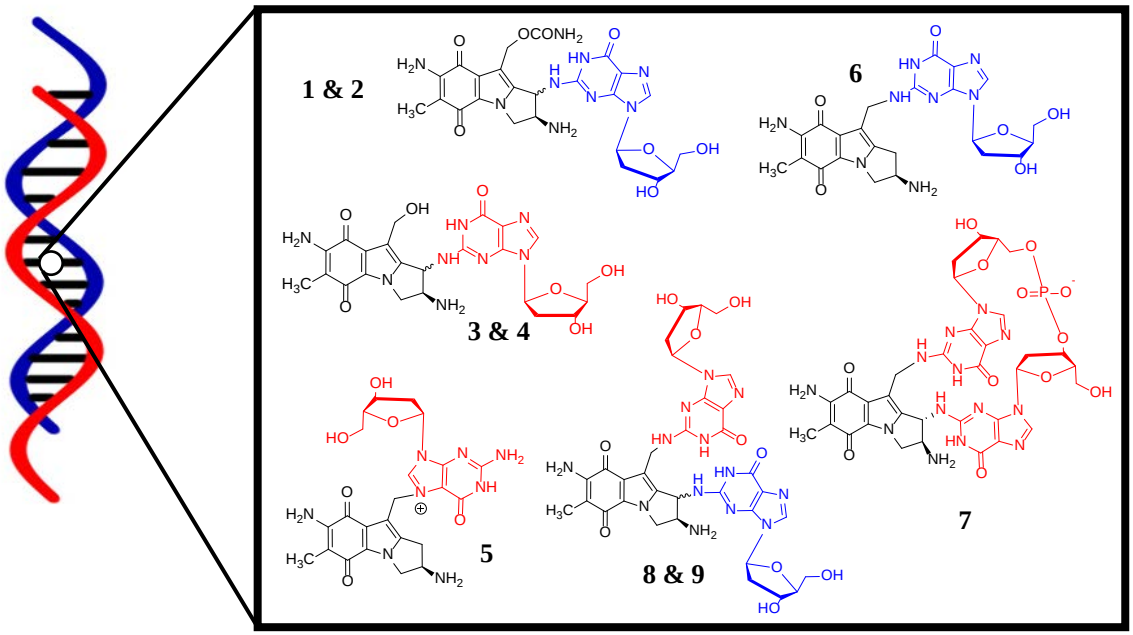

	Mono-adducts		Bis-adducts
1	1,2-*trans*-deoxyguanosine monoadduct	**6**	N2 2,7-diaminomitosene monoadduct
2	1,2-*cis*-deoxyguanosine monoadduct	**7**	dG-dG intrastrand cross-link
3	1,2-*trans*-deoxyguanosine decarbamoyl monoadduct	**8**	1,2-*trans*-dG-dG interstrand cross-link
4	1,2-*cis*-deoxyguanosine decarbamoyl monoadduct	**9**	1,2-*cis*-dG-dG interstrand cross-link
5	N7 2,7-diaminomitosene monoadduct		

Figure 1.6 Structures of nine characterized DNA adducts resulting from MC treatment.[11,32]

The formation of ICLs is considered the main cause of cellular toxicity. ICLs are extremely potent, with the ability to produce cell death with as little as one cross-link per genome.[17-20] The mitomycins ability to form ICLs revealed that covalent linkage of complementary strands occurred only in the presence of cell lysates or other exogenous reductants, thus suggesting that mitomycins must first undergo reductive activation prior to formation of the lethal DNA cross-links.[17-19]

Mitomycin reduction can occur via one or two electron reduction processes initiated through enzymatic or chemical means. Chemically, MC has been shown to become reductively activated by thiols, dithiols, ascorbic acid, formate radicals, sodium

borohydride, sodium dithionite, and platinum catalyzed hydrogenation.[19,39-41] In addition to the previous chemicals, reductive activation of MC has been reported to occur appreciably through an acid catalyzed pathway at a pH < 5.[42] Two electron reduction of MC is accomplished by DT-diaphorase, yielding the hydroquinone mitomycin.[43] The most common enzyme catalyzed reduction occurs via one electron by NADPH-cytochrome P-450 reductase, xanthine oxidase, NAD(P)H-cytochrome c reductase, xanthine dehydrogenase, and NADH-cytochrome b_5 reductase.[11,43-45]

Upon discovering that mitomycins must first be reductively activated, Iyer and Szybalski suggested a preliminary reduction pathway using the resonant forms of mitomycins (Figure 1.7).[17-19] Briefly, their proposal began with a reduction of the quinone ring (**1**) to a hydroquinone moiety (**2**), followed by an elimination of the methoxy (hydroxyl) group at carbon 9a (**3**), and proton removal from carbon 9. This results in the formation of an aromatic indole system (**4**).[17,18]

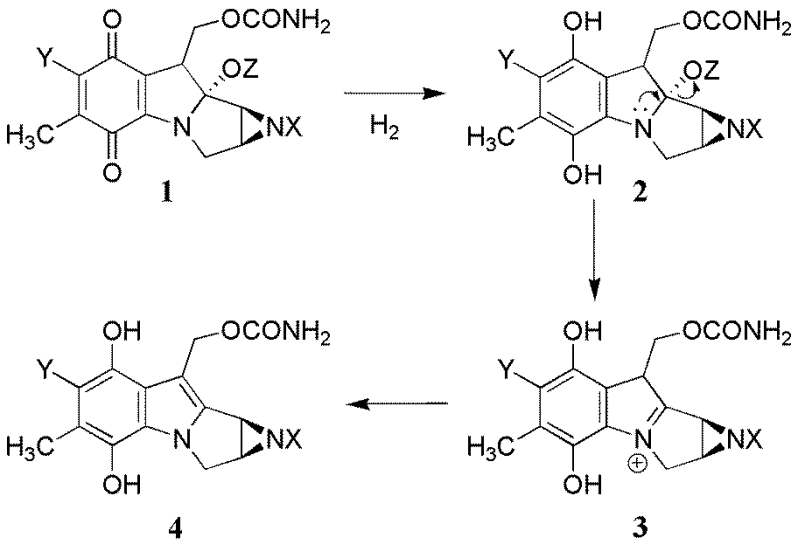

Figure 1.7 Reductive activation of mitomycins presented by Iyer and Szybalski.[18]

Further inquiry into the mechanism of reductive activation has afforded the most widely accepted pathway towards activation of C1 and C10 for DNA alkylation (Figure 1.8), presented by the Tomasz research group in 1997.[32] This pathway includes the formation of mono and bis-alkylated species and reduction via one or two electron routes. Initial reduction of the mitomycin quinone (MC) can occur via one or two electrons yielding a semiquinone (**5**) or a hydroquinone (**6**), respectively.

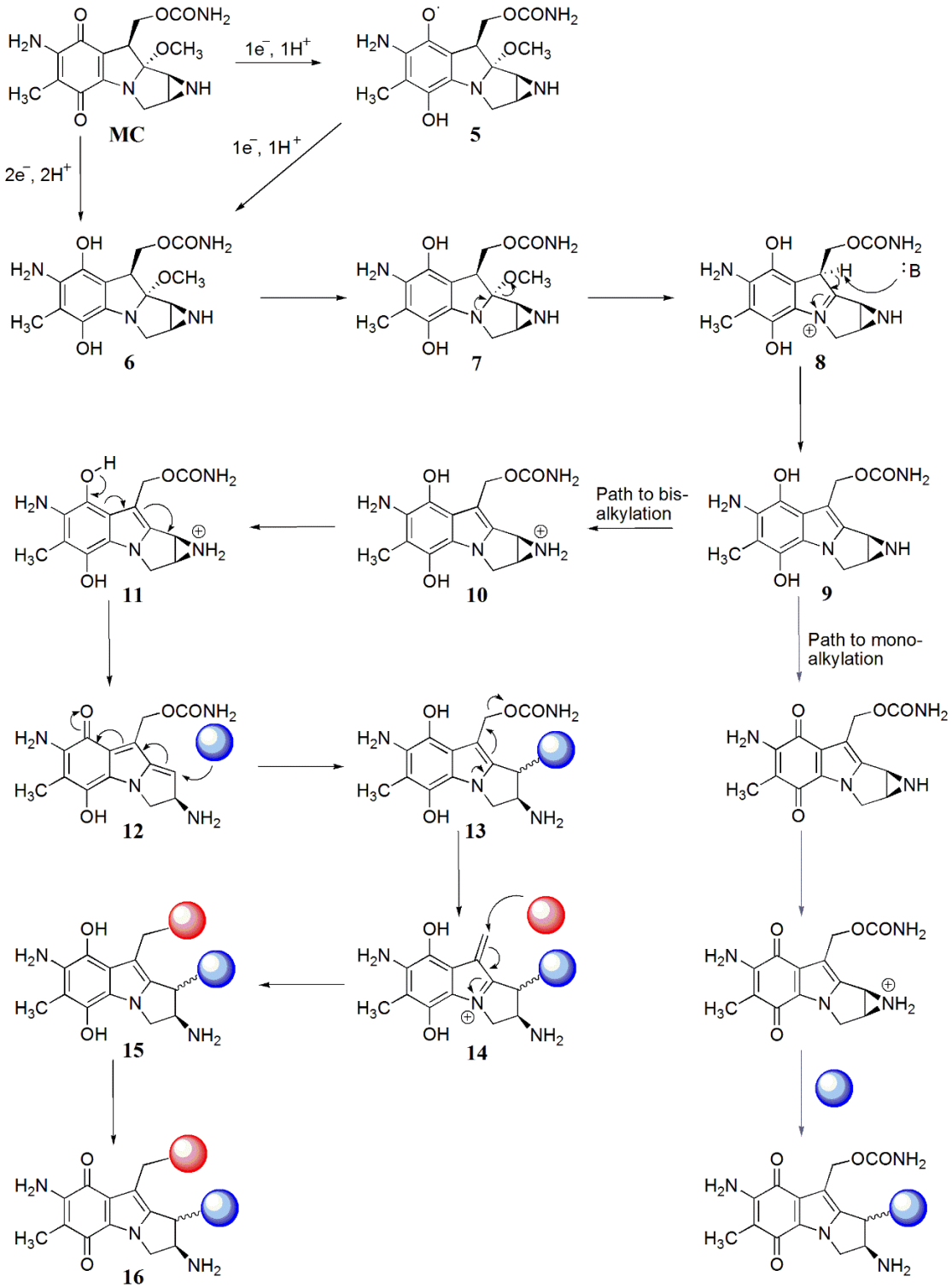

Figure 1.8 Mitomycin C reductive activation cascade leading to mono and bis-alkylation. The blue sphere acts as the first nucleophile, whereas the red sphere is the second nucleophile completing the DNA interstrand cross-link.[11,32]

From the hydroquinone (**6**), elimination of the methoxy group (**7**) occurs via formation of an N4 iminium intermediate (**8**). Deprotonation at C9 leads to formation of the leucoaziridinomitosene (**9**). At this point, the leucoaziridinomitosene can continue towards formation of a bis-adduct or undergo mono-alkylation. In route to creating the interstrand cross-link, the leucoaziridinomitosene (**9**) is protonated to form the aziridinium (**10**). The resonance stabilized aziridine ring opening occurs at C1, forming a quinone methide (**12**), via **11**. From here, nucleophilic attack of the exocyclic amino group of guanosine, as represented by the blue sphere, upon C1 of **12** leads to the first DNA alkylation event (**13**). After alkylation at C1, elimination of the carbamate group (**14**) produces the second electrophilic site on C10. The second alkylation event occurs through nucleophilic addition of the complimentary strand's guanine exocyclic N2 amino group (red sphere) producing the bis-alkylated DNA adduct (**15**). Subsequent oxidation of the hydroquinone to the quinone produces the final mitomycin-DNA interstrand cross-link (**16**), which have been characterized by HPLC and LC-MS/MS analysis.[7,10-12,32,37]

Mitomycin C Oxidative Stress

Quinone containing compounds that are capable of undergoing one or two electron redox processes, such as MC, can lead to the increased production of reactive oxygen species (ROS) in the presence of molecular oxygen.[46] ROS play integral roles in the normal physiological processes of cells at normal levels, including cell signaling and combating infectious agents.[47] At elevated levels, ROS participate in oxidative stress or damage intracellularly, leading to disruption of normal function and potential damage to lipids, DNA, mitochondria, and proteins.[47-49] The quinone-containing mitomycins undergo this one or two electron reduction with several oxidoreductase enzymes in route

to alkylating DNA. Inquisitions into the MC related increase in chromosomal abberations, chromatid rearrangements and fragmentations, and additional DNA damage were directed towards the drug induced production of ROS and its relationship to these effects.[17,56,57]

Early *in vitro* studies into the mitomycin-mediated formation of ROS identified the generation of hydrogen peroxide, hydroxyl radicals, and superoxide anion by reduced MC (Figure 1.9).[52-58] Identification of MC induced superoxide anion was conducted using sulfite oxidation in microsome NADPH oxidase systems.[52] Through inhibition of sulfite oxidation in the presence of superoxide dismutase, superoxide anion was identified as a result of MC reduction in the presence of oxygen.[52] Additional evidence to the mitomycin catalyzed superoxide production was conducted using electron spin resonance (ESR) and the spin trapping reagent N-*tert*-butyl-α-phenylnitrone.[54] The identity of each species was determined with the addition of catalase and superoxide dismutase to the reaction mixture, leading to a loss of the spin trap nitroxide radical. These results further indicated that reduced MB and MC produce superoxide anion and hydrogen peroxide.[54] Both MC and a MC-DNA complex were found to generate hydrogen peroxide after reduction followed by exposure to air. Hydrogen peroxide levels were abolished upon addition of catalase to the reaction mixture of both MC species, confirming the identity of the ROS as H_2O_2.[53] Characterization of hydroxyl radical formed by enzymatically reduced MC was conducted using ESR and a spin trapping agent.[51,55] Hydroxyl radical identification was confirmed using the addition of superoxide dismutase and catalase, as well as the formation of ethylene from methional.[55] The generation of ROS through

reduced MC was found to lead to the induction of single strand cleavages in PM2 covalently closed circular DNA, thyroid, plasmid, and λ DNA.[50,51]

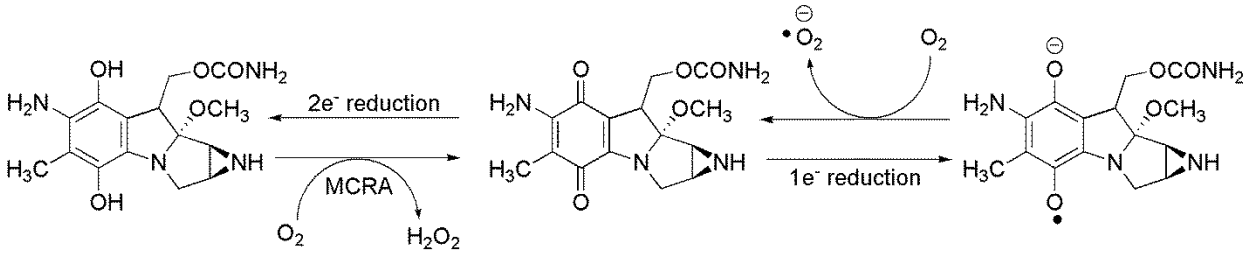

Figure 1.9 Schematic of MC induced ROS production. One or two electron reduced MC leads to the production of superoxide anion or hydrogen peroxide in the presence of molecular oxygen.[8]

Exploration into the correlations between cytotoxicity of mitomycins and the production of ROS was investigated using cellular systems. Comparisons of four mitomycin compounds (MC, porfiromycin, BMY-25282, and BL-6783) and their associative cytotoxicity were conducted in EMT6 tumor cells under an aerobic environment (Figure 1.10).[59] Using EMT6 cell sonicates, NADPH-cytochrome c reductase, xanthine oxidase, and bovine heart mitochondria as biological reduction systems, the consumption of oxygen by the four compounds was measured. In aerobic conditions, BMY-25282 and BL-6783 displayed increased toxicity over both MC and porfiromycin. Generation of both hydroxyl and superoxide radicals were greater for BMY-25282 and BL-6783 than MC and porfiromycin in three of the four reduction conditions, providing indications that enhanced aerobic toxicity is likely affiliated with increased production of ROS by mitomycins.[59]

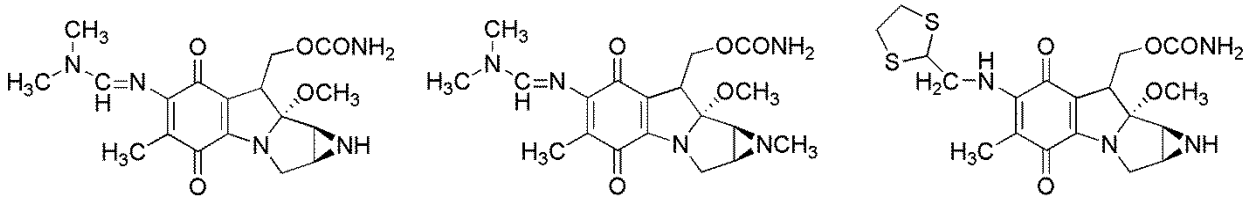

BMY-25282 BL-6783 BMY-43324

Figure 1.10 Structural depictions of mitomycin analogs: BMY-25282, BL-6783, BMY-43324.[59,63]

Experiments conducted with VA-13 and IMR-90 human embryonic cells provided additional insight into the role of ROS.[60] Specifically, VA-13 cells, which are more sensitive to oxygen radical production than are IMR-90 cells, were more susceptible to MC treatment. A similar frequency in cross-linking was displayed between cell lines, although increased levels of double strand DNA breaks were observed in VA-13 cells. Pre-incubation with superoxide dismutase or catalase led to an increased survival of VA-13 cells upon treatment with MC but not in IMR-90 cells, suggesting that sensitivity to MC treatment could be correlated with the ability to neutralize ROS.[60]

Mitomycin Anaerobic Preference

In the presence of molecular oxygen, reductive activation of MC is halted, returning it back to the inactive quinone form.[17-19, 56-57] This subsequent reduction-oxidation pathway renders MC less potent in O_2 rich environments, decreasing the ability to form ICLs, with increased production of reactive oxygen species.[61] As a result, in the early 1980s, the potential of MC as a selective hypoxic anti-tumoral drug was investigated. Measurements of MC metabolism (the rate of MC disappearance and formation of an alkylating species) were conducted in EMT6 and S-180 cell sonicates under hypoxic and aerobic conditions. These studies found that the rate of MC metabolism was much greater under hypoxia than in the presence of oxygen.

Additionally, EMT6 cells treated with MC anaerobically exhibited increased sensitivity to the drug.[61] Investigations were expanded into the exploration of porfiromycin cytotoxicity to EMT6 cells under anaerobic and aerobic conditions. Porfiromycin displayed similar cytotoxicity to MC under hypoxia, but had diminished activity compared to MC towards EMT6 cells in the presence of oxygen, establishing the notion that MC and porfiromycin are selective hypoxic agents.[62]

Mitomycin analogues BMY-25282, BMY-43324, and BL-6783 were evaluated for their preference to anaerobic versus aerobic environments in EMT6 cells (Figure 1.10). BMY-43324 displayed hypoxic preference, with greater cytotoxicity and cross-link formation than MC and porfiromycin. BL-6783 experienced no difference in toxicity under hypoxic or aerobic conditions. Under aerobic conditions, BMY-25282 displayed an increased potency and earliest formation of DNA cross-linking. Structural analysis (MC vs. porfiromycin; BMY-25282 vs. BL-6783) with ICL formation and cell killing ability revealed that methylation of the aziridine nitrogen leads to a preference towards hypoxic conditions.[63]

Mitomycin C Resistance

Effective MC treatment relies upon tumors that are high in flavin reductases and other proteins that activate mitomycins.[8] Inspections into the cytotoxic resistance of mitomycin producing *Streptomyces lavendulae* identified two genes (mcrA and mcrB) responsible for coding the protein MCRA (mitomycin C resistance associated). This protein contains a covalently linked FAD, assisting in the reoxidation of hydroquinone mitomycin C to the quinone moiety in the presence of oxygen. Sequential analysis of MCRA revealed similarities to oxygen oxidoreductases in animal, plant, and bacterial

organisms.[64,65] Expression of the mcrA gene into CHO cells lead to a substantial increased resistance to mitomycin C and porfiromycin under aerobic conditions. When treated under hypoxic conditions, a slight increase in resistance was observed in the MCRA-1 expressing CHO cells. MCRA and its sequential relationship to oxygen oxidoreductase enzymes in animal cells generates a plausible stance that tumor cells exhibiting overexpression of these enzymes could lead to increased resistance to MC.

The necessity of biological reduction to form ICLs allows for the ability to develop resistance to mitomycin treatment. Multiple cancer cells lines have been shown to exhibit resistance to MC, in accordance with the regulation of several bioactivating enzymes, including DT-diaphorase and NADPH:cytochrome c oxidoreductase.[66-68] The ability to re-establish MC sensitivity was displayed in CHO cells expressing the MC resistant MCRA protein through overexpression of DT-diaphorase and NADPH:cytochrome c oxidoreductase.[68]

Attempts to profile genes involved in MC resistance were carried out through nonessential gene deletions in *Saccharomyces cerevisiae*. Deletions of genes involved in nucleotide excision repair, including damage recognition (RAD14 and RAD4) and incision endonucleases (Radp1-Rad10p complex and Rad2p) led to an increased sensitivity of MC. Further increased sensitivity to MC was observed upon deletion of the PSO2/SNM1 gene, which is involved in the repair of interstrand cross-links. Lastly, the removal of multiple DNA damage checkpoint genes led to an increase in yeast's sensitivity to MC.[69]

Successful utilization of MC moving forward appears to be dependent on a variety of aforementioned factors. These factors include the enzymatic profile of cells,

their ability to reduce MC, and presence of resistant genes. For these reasons, future uses of MC as an effective treatment option may require tailoring to the appropriate system.

Aziridinomitosene Biological Activity

Investigations into the biological activity of AZMs have been limited in comparison to the mitomycins. The inaugural explorations into the biological activity of AZMs were conducted through the conversion of MB and NMA to their respective AZMs (Figure 4).[21,70-74] *In vitro* examinations revealed that NMA-AZM and MB-AZM exhibit powerful broad spectrum bactericidal agent in accordance with the mitomycins, while showing additional activity in mice orally and subcutaneously against *Staphylococcus aureus* and *Streptococcus pyogenes* C-203.[21]

In 1971, Kinoshita and co-workers studied the biological activity of the five AZMs depicted in Figure 1.11. Evaluations of the bactericidal and anti-tumor activity of NMA-AZM and multiple mitosene compounds demonstrated that the most active compounds contained the three functional groups: an aziridine ring, carbamate, and quinone. NMA-AZM displayed activity against gram positive and gram negative bacteria, while also demonstrating high anti-tumor activity against solid sarcoma 180.[21,72-74]

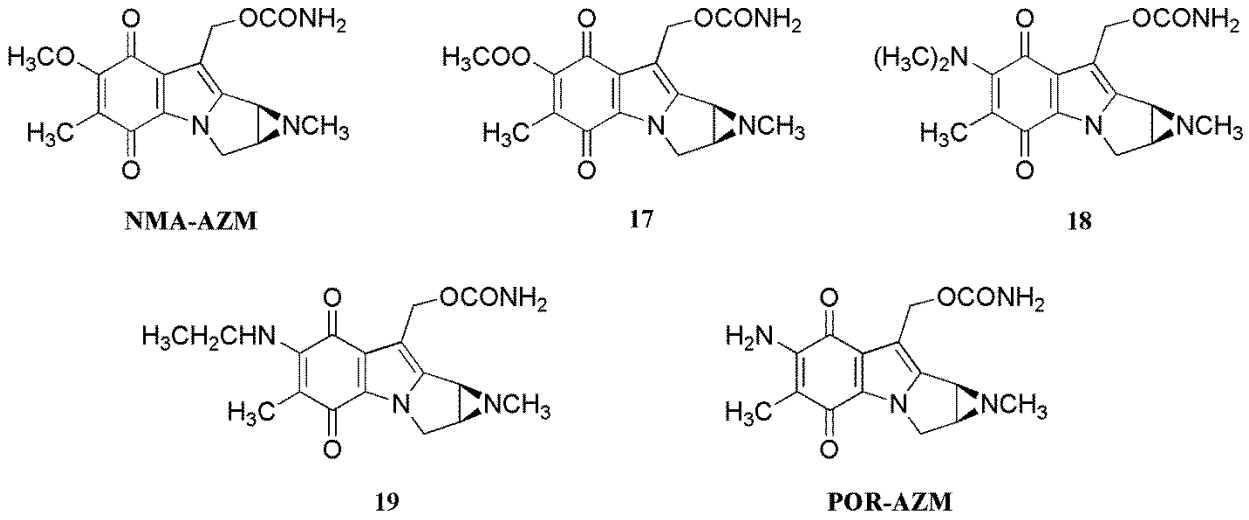

Figure 1.11 Structures of aziridinomitosenes studied by Kinoshita and co-workers.[72]

The other AZMs (17, 18, 19, POR-AZM) were evaluated for their bactericidal properties against gram positive and gram negative bacteria, but not for their anti-tumoral activity. Of these, **18** (7-dimethylamine) displayed similar activity against gram positive bacteria to NMA-AZM, with decreased efficacy towards gram negative bacteria. POR-AZM and **19** showed little efficacy as a bactericidal.[72]

Hodges and Remers evaluated the biological activity of NMA-AZM in P-388 murine leukemia with several other mitosene analogs with various substitutions about carbon 1.[73] Their studies found that NMA-AZM was more effective at prolonging life in treated mice over those treated with any of the 1-substituted mitosenes. When compared to MC, NMA-AZM was found to have a higher optimal dose at 12.8 mg/kg versus that of 3.2 mg/kg for MC. However, NMA-AZM was found to be more effective at increasing the life span of treated mice, despite its requirement for higher dosages.[73]

The synthesis and subsequent anti-tumor activity against P-388 leukemia in mice of ten different 7-substituted AZMs was conducted by Iyengar, Remers, and Bradner

(Figure 1.12).[74] Several of the synthetic AZMs showed activity against the murine tumors comparable to MC, but required higher dosages. The most active AZMs, NMA-AZM, and **25** were both successful at prolonging the life span of treated mice over that of MC. The observed increase in survival time required four and eight fold greater dosages, respectively. AZM **21** provided the only mice surviving to 30 days after treatment, in two dosages, both of which were higher than MC (8x and 16x). Furthermore, activity was seen at high dosages by **22** and **26**; there was not an observed increase in survival times compared to MC treated mice. [74]

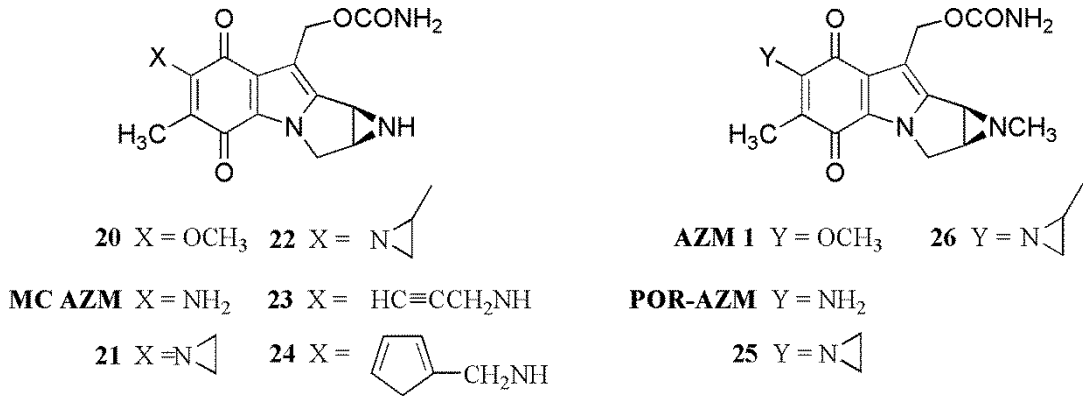

Figure 1.12 Structural representations of 7-substituted aziridinomitosenes.[74]

Investigations into the range of activity displayed the 7-substituted AZMs was conducted by testing **MC-AZM**, **22**, **23**, and MC against mice inoculated with L-120 murine leukemia. Activity was seen in two of the compounds (AZM **22** and **23**), but not to the extent of MC. Of particular interest was the inactivity MC-AZM, as it is an intermediate in the DNA alkylation pathway and would have thought to present as an active compound.[74]

Additional analysis into the biological activity exhibited by the 7-substituted AZMs was an assessment of the structural elements leading to increased potency. A key

distinguishing feature between the two sets of AZMs is the presence of a methylated aziridine ring in NMA-AZM, POR-AZM, **25**, and **26**. This was found to increase the activity of the carbon 7-substituted AZMs in accordance with the calculation of a minimum effective dose (MED), the minimum dose to exhibit a response. Explanations into the increased activity observed by N-methylated AZMs were attributed to the increased basicity of the aziridine. Protonation of the aziridine ring leads to activation and ring opening, followed by subsequent nucleophilic addition at C1. Therefore, a methylated aziridine ring would have increased basicity when compared to the hydrogenated version, leading to greater anti-tumoral activity in AZMs.[74] In addition, the presence of the aziridine ring functional group was affiliated with the ability to prolong life by NMA-AZM treated mice inoculated with P-388 leukemia.[73]

Several AZMs have displayed biological activity with most requiring elevated quantities above MC in order to elicit similar responses. Despite the increased dosages, treatment with some AZMs resulted in the prolongation of life. Further, the increased activity of methylated AZMs suggests that synthetic efforts should consider incorporating this functional group into their architecture.

Aziridinomitosene DNA Alkylation

Formation of DNA ICLs have been attributed as the main cause of the cytotoxicity associated with mitomycins.[20,33] Exploration into the pathway through which mitomycins generate ICLs, incorporates AZMs as intermediates towards DNA alkylation.[32] Investigations in DNA modification of AZMs began with AZMs, which were converted from their parent mitomycins through reduction-oxidation reactions and

DNA (Figure 1.13).[75,76] Soon after, evaluations of a C6/C7 unsubustituted synthetic AZM (H/H-AZM) and its ability to covalently modify DNA were investigated.[77,78]

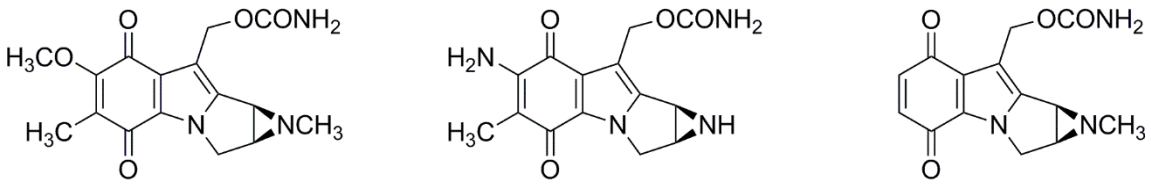

Figure 1.13 Structure of AZMs investigated for DNA alkylating properties. NMA-AZM, MC-AZM, and (1S, 2S)-6-desmethyl(methylaziridino)mitosene (H/H-AZM).[75-79]

Teng and coworkers conducted an *in vitro* ICL analysis using MC, NMA, and NMA-AZM under hypoxic conditions in the presence of the reducing agent sodium dithionite and radiolabeled DNA.[75] Results showed that NMA-AZM exhibits a sequence selectivity towards 5'-XCpGY, similar to NMA and MC, while cross-link formation by NMA-AZM occurred at higher percentage towards the 5'-XCpGY-3' motif than MC at pH 4.5 and 7.5, with similar frequency in 5'-XGpCY-3' sequences. The cross-link percentages for NMA-AZM were consistent with that of its parent mitomycin, NMA, throughout the study.[75]

Additional studies into AZM DNA alkylation were conducted using the UvrABC assay in the absence of a reducing agent, with NMA-AZM and MC-AZM.[76] Under non-reducing conditions, AZMs displayed similar sequence specificity to reduced MC, bonding preferentially to the 5'-CpG site, with alkylation occurring at the guanine residue, as in the previous study.[75,76] Furthermore, upon reductive activation of NMA-AZM with sodium dithionite, a decline of sequence selectivity of DNA alkylation was observed, suggesting an increase in the reactivity of this species.[76]

The DNA modifying capabilities of the C6/C7 unsubstituted AZM, (1S, 2S)-6-desmethyl(methylaziridino)mitosene (H/H-AZM), were also evaluated using the UvrABC assay.[78] In the absence of reducing agent, H/H-AZM formed DNA cross-links with selectivity towards both 5'-CpG and 5'-TpG sequences, with modifications occurring at guanine residues. Cross-linking with H/H-AZM was shown to be time dependent with increased formation at longer incubation times ranging from 1-4 hours. In addition to the DNA modifying properties of H/H-AZM, evidence was provided that H/H-AZM could be forming DNA-protein cross-links (DPCs). Formation of DPCs is highly likely given the electrophilic sites located at carbon 6 and carbon 7, in addition to the traditional C1 and C10 locations of DNA alkylation in mitomycins.[78]

DNA binding studies with H/H-AZM were conducted in vitro with the absence of exogenous reductants under aerobic conditions, revealing formation of DNA ICLs with preference to a 5'-CpG motif.[79] The cross-linking ability was evaluated as a function of pH from 5-7.5, exhibiting the largest formation of ICLs at pH 6.0. These results appear to be consistent with the increased toxicity displayed by MC in acidic environments. Alterations in the levels of interstrand cross-linking were seen based on the nucleotide immediately preceding and following the 5'-CpG sequence, with the highest ICL formation occurring in the presence of the tetranucleotide sequence of 5’-ACGT. Replacement of 2'-deoxyguanosine for 2'-deoxyinosine, led to abolishment of cross-link formation, confirming the critical role the exocyclic amino group of 2'-deoxyguanosine in ICL formation.[79]

These studies provide direct evidence that AZMs are capable of forming DNA ICLs, and do so with similar properties to MC. AZM-induced ICL formation was found

to follow the same sequence specificity of MC with preference towards 5'-CpG-3' motifs. Furthermore, DNA alkylation was found to occur at the guanine residues, as displayed by MC. DNA modification by AZMs has been shown to occur with similar frequency as MC, in the presence and absence of exogenous reductants, proposing that formation of AZM DNA adducts may not require reductive activation.

Aziridinomitosene Analogs

A number of AZM analogues have been synthesized but little on their biological activities have been published to date (Figure 1.14). In 1996, an analog to the MA AZM was synthesized by the Jimenez group. The synthesis started with nitration of 2,5-dimethylanisole. Their final product (**27**) lacked a carbamate functional group, and a functional group at the C10 position altogether.[80] Soon after, a fully functional MA AZM was synthesized, containing both the aziridine ring and carbamate groups.[81]

Following this reports of a successful synthesis of a tetracyclic model for an aziridinomitosene, via an 11 step synthesis were published.[82] This process originated with the *D*-erythronolactone derivative (-)-2,3-*O*-isopropylidene-*D*-erythronolactone. The final two products consisted of the aziridinomitosene analog possessing an ester at C10, with an unprotected aziridine (**28**) or the N-phosphorylated analog (**29**).[82]

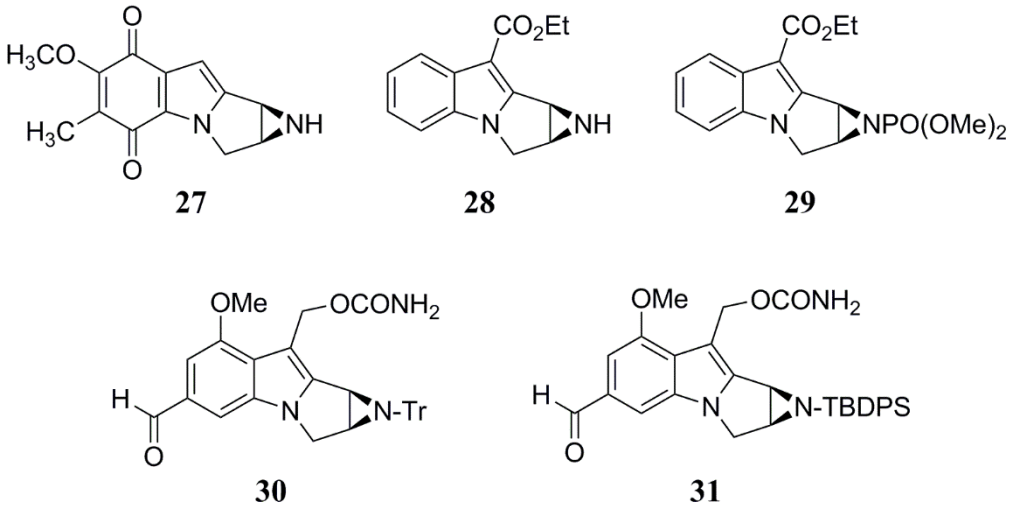

Figure 1.14 Structures of synthetic AZM analogs.[80,82,83]

Later, Wiedner and co-workers synthesized two protected (N-trityl (**30**) and N-TBDPS (**31**)) derivatives of the AZM version of FK317, and evaluated their ability to undergo solvolysis at carbons 1 and 10.[83] Under mild nucleophilic conditions, the analogues **30** and **31** exhibited a faster heterolysis at C10 than C1. This observation presents with conflicted behavior to that of typical AZMs containing the stabilizing quinone ring, creating C1 as the preferential electrophile to nucleophilic attack.[83]

In 2011, Bonham and co-workers successfully synthesized a diazole analogue (**32**) of an aziridinomitosene, fusing an aziridine ring onto a pyrrolo[1,2-a]benzimidazole, and evaluated its biological activity (Figure 1.15). An additional heterocyclic system, *N*-[(1-tritylazridin-(2S)-yl)methyl]-1*H*-benzimidazole (**33)** was also synthesized and studied in this report. The cytotoxicity of these compounds were evaluated against MC in three cell lines, GM00637 (human normal skin fibroblasts) and two human breast cancer cell lines (MCF-7 and HCC1937 (*BCRA1* deficient)).[84]

32 **33**

Figure 1.15 Structural representations of synthetic AZM analogs 32 and 33. Aziridine ring fused onto a pyrrolo[1,2-a]benzimidazole (32) *N*-[(1-tritylazridin-(2S)-yl)methyl]-1*H*-benzimidazole (33).[84]

The synthetic compounds **32** and **33** showed lower toxicity in the GM00637 cell lines than MC with IC_{50} values of 3.11 ± 0.44, 1.26 ± 0.13, and 0.77 ± 0.18 μM respectively, while **33** displayed the largest potency over **32** and MC in MCF-7 cells with a IC_{50} of 0.22 ± 0.04, 0.84 ± 0.14, and 0.93 ± 0.11 μM, respectively. In HCC1937 cells, MC was the most potent with an IC50 value of 0.03 ± 0.01 μM, followed by **33** (0.16 ± 0.03 μM), and finally **32** (0.67 ± 0.01 μM). Both analogs have preferential toxicity towards breast cancer cell lines (MCF-7 and HCC1937) over that of normal human skin fibroblasts (GM00637).[84]

Aziridinomitosenes: Potential Problems

To date, there has been very limited investigations into aziridinomitosenes and their potential biological activity when compared to the mitomycins. Most of the exploration has been oriented towards AZMs derived from the conversion of the parent mitomycin, somewhat restricting functionalization and potential improvements in the cytotoxicity of the molecules. One likely main cause of the deficiency in attention is due to the difficulty in synthesizing AZMs and their analogs while maintaining functionality, natural substitution pattern about the tetracyclic core, and correct stereochemistry.[77,82] The presence of the double bond between carbons 9 and 9a allows for allylic like stabilization of carbon 1 upon opening of the aziridine ring. This intermediate occurs in

the reductive activation of mitomycins and their path towards DNA alkylation. In the case of AZMs, it produces a reactive species capable of readily undergoing solvolysis.[71,77] Han and Kohn showed that AZMs derived from MC and porfiromycin undergo methanolysis with half-lives as low as three and fourteen minutes at a pH of 7.0, respectively.[71] Similar studies were conducted with H/H-AZM at 20 ºC and at a pH of 7.0, the half-life was found to be 2,000 minutes, over 660 fold greater than MC-AZM.[78] The major deviation in observed half-life was stated to likely be attributed to the presence of the electron donating amine present at C7 of MC-AZM and POR-AZM. Increased electron density within the indoloquinone system presumably assists in stabilizing carbocation formation at C1, leading to increased reactivity and susceptibility to solvolysis.[78]

In addition to the difficulties presented in synthesizing AZMs, their biological activities have shown promise but have not yet been shown to surpass that demonstrated by MA or MC. Several AZMs have displayed bactericidal activity and anti-tumoral properties similar to the mitomycins. Despite this similar activity, the efficacy of AZMs investigated required larger dosages than MC or MA to exhibit a similar response.[21,72-74]

Potential Benefits of Aziridinomitosenes over Mitomycins

DNA alkylation by MC is reliant upon reductive activation; AZMs do not share this requirement in their ability to alkylate DNA, presumably affording AZMs an advantage as a DNA modifying agent.[17-19] Decreased sensitivity to MC has been documented in cells lines lacking or expressing decreased levels of oxidoreductase enzymes acting in the reductive activation cascade of MC.[66-68] As such, mutations or alterations in cancer cells can lead to changes in the successful utilization of MC,

rendering tumors more or less sensitive to treatment based on the expression of these reductive activation enzymes. AZM activity may not rely upon the levels of these enzymes, establishing the hypothesis that they may be more efficacious with decreased dependency on oxidoreductase enzymes in their biological activity. Furthermore, investigations into AZM DNA alkylation produced similar frequencies in the ICL formation under aerobic conditions. This may lead to a broad spectrum anti-tumoral agent that can be applied to several environments, rather than acting as a selective hypoxic agent like MC.

Studies with substitutions at C7 within MA and MC have presented evidence that increased lipophilicity leads to more cytotoxic compounds.[85] The ability to fine tune functional groups at C6, C7, and C10 within AZMs presents with the potential to create compounds with a more facile ability to traverse cellular membranes and increase stability of the electrophilic carbons, and potentially rendering them more potent.

Concluding Remarks

Multiple AZMs have been found to exert antibiotic and anti-tumoral activities similar to mitomycins. Of particular interest is an observed prolongation of life in mice treated with three AZM analogs over that of those that were MC treated. Regeneration in the interest of AZMs could prove to be valuable in the search for new antibiotics or chemotherapeutic agents with a decrease in serious side effects. Despite the difficulties faced in synthesizing these compounds, there have been many successful attempts in producing AZMs. Their efforts allow for further modification and “fine-tuning” to enhance AZM biological activity. Moving forward, a focus should be directed towards enhancing the lipophilicity of AZMs for enhanced cellular uptake, the steric and

electronic effects of substituents located at C6 and C7, and methylation of the aziridine nitrogen.

References

1. Hata, T.; Sano, Y.; Sugawara, R.; Matsumae, A.; Kanamori, K.; Shima, T.; Hoshi, T. Mitomycin, A New Antibiotic From Streptomyces. I. *J. Antibiot.; Ser. A.* **1956**, *9*, 141-146.
2. Kanamori, H.; Shima, T.; Morita, C.; Hata, T. Studies on Antitumor Activity of Mitomycin. *J. Antibiot.; Ser. A.* **1957**, *10*, 120-127.
3. Wakaki, S.; Marumo, H.; Tomioka, K.; Shimizu, G.; Kato, E.; Kamada, H.; Kudo, S.; Fujimoto, Y. Isolation of New Fractions of Antitumor Mitomycins. *Antibiot. Chemother.* **1958**, *8*, 228-240.
4. Herr, R. R.; Bergy, M. E.; Eble, T. E.; Jahnke, H. K. Porfiromycin, a new antibiotic II. Isolation and Characterization. *Antimicrob. Agents Annu.* **1960**, *1*, 23-26.
5. Tomasz, M. Mitomycin C: small, fast and deadly (but very selective). *Chem. Biol.* **1995**, *2*, 575-579.
6. Danishefsky, S. J.; Schkeryantz, J. M. Chemical Explorations Driven by an Enchantment with Mitomycinoids – A Twenty Year Account. *Synlett* **1995**, 475-490.
7. Rajski, S. R.; Williams, R. M. DNA Cross-Linking Agents as Antitumor Drugs. *Chem. Rev.* **1998**, *98*, 2723-2795.
8. Galm, U.; Hager, M. H.; Van Lanen, S. G.; Ju, J.; Thorson, J. S.; Shen, B. Antitumor Antibiotics: Bleomycin, Enediynes, and Mitomycin. *Chem. Rev.* **2005**, *105*, 739-758.
9. Andrez, J.-C. Mitomycins syntheses: a recent update. *Beilstein J. Org. Chem.* **2009**, *5*, doi:10.3762/bjoc.5.33.
10. Remers, W. A. *Anticancer Agents from Natural Products*, 2nd ed.; CRC Press.
11. Paz, M. M.; Pritsos, C. A. Chapter Seven. The Molecular Toxicology of Mitomycin C. *Adv. Mol. Toxicol.* **2012**, *6*, 243-299.
12. Bass, P. D.; Gubler, D. A.; Judd, T. C.; Williams, R. M. Mitomycinoid Alkaloids: Mechanism of Action, Biosynthesis, Total Synthesis, and Synthetic Approaches. *Chem. Rev.* **2013**, *113*, 6816-6863.
13. Webb, J. S.; Cosulich, D. B.; Mowat, J. H.; Patrick, J. B.; Broshard, R. W.; Meyer, W. E.; Williams, R. P.; Wolf, C. F.; Fulmor, W.; Pidacks, C.; Lancaster, J.

E. The Structures of Mitomycins A, B and C and Porfiromycin-Part I. *J. Am. Chem. Soc.* **1962**, *84*, 3185-3187.

14. Webb, J. S.; Cosulich, D. B.; Mowat, J. H.; Patrick, J. B.; Broshcard, R. W.; Meyer, W. E.; Williams, R. P.; Wolf, C. F.; Fulmor, W.; Pidacks, C.; Lancaster, J. E. The Structures of Mitomycins A, B, and C and Porfiromycin – Part II. *J. Am. Chem. Soc.* **1962**, *84*, 3187-3188.
15. Tulinsky, A. The Structure of Mitomycin A. *J. Am. Chem. Soc.* **1962**, *84*, 3188-3190.
16. Kojima, H.; Takahata, C.; Lemin, D.; Takahaski, M.; Kumamoto, T.; Nahanishi, W.; Suzuki, N.; Ishikawa, T. Synthesis of the Aziridinomitosene Skeleton by Application of Guanidinium Ylide-Mediated Aziridination. *Helveta Chimica Acta* **2013**, *96*, 379-388.
17. Iyer, V. N.; Szybalski, W. A Molecular Mechanism of Mitomycin Action: Linking of Complementary DNA Strands. *Proc. Natl. Acad. Sci. U.S.A.* **1963**, *50*, 355-362.
18. Iyer, V. N.; Szybalski, W. Mitomycins and Porfiromycin: Chemical Mechanism of Activation and Cross-linking of DNA. *Science*, **1964**, *145*, 55-58.
19. Szybalski, W.; Iyer, V. N. Crosslinking of DNA by enzymatically or chemically activated mitomycins and porfiromycins, bifunctionally “alkylating” antibiotics. *Fed. Proc.* **1964**, *23*, 946-957.
20. Palom, Y.; Kumar, G. S.; Tang, L.-Q.; Paz, M. M.; Musser, S. M.; Rockwell, S.; Tomasz, M. Relative Toxicities of DNA Cross-Links and Monoadducts: New Insights from Studies of Decarbamoyl Mitomycin C and Mitomycin C. *Chem. Res. Toxicol.* **2002**, *15*, 1398-1406.
21. Patrick, J. B.; Williams, R. P.; Meyer, W. E.; Fulmor, W.; Cosulich, D. B.; Broshard, R. W.; Webb, J. S. Aziridinomitosenes: A New Class of Antibiotics Related to the Mitomycins. *J. Am. Chem. Soc.* **1964**, *86*, 1889-1890.
22. Crooke, S. T.; Brander, W. T. Mitomycin C: a review. *Cancer Treat. Rev.* **1976**, *3*, 121-139.
23. Bradner, W. T. Mitomycin C: a clinical update. *Cancer Treat. Rev.* **2001**, *27*, 35-50.
24. Verweij, J.; Pinedo, H. M. Mitomycin C: mechanism of action, usefulness and limitations. *Anti-Cancer Drugs* **1990**, *1*, 5-13.
25. Doll, D. C.; Weiss, R. B.; Issell, B. F. Mitomycin: Ten Years After Approval for Marketing. *J. Clin. Oncol.* **1985**, *3*, 276-286.
26. Abraham, L. M.; Selva, D.; Casson, R.; Leubovitch, I. Mitomycin. Clinical Applications in Ophthalmic Practice. *Drugs* **2006**, *66*, 321-340.

27. Physicians' Desk Reference, 29th ed.; Medical Economics Company: Oradell, 1975.

28. Santhiago, M. R.; Netto, M. V.; Wilson, S. E. Mitomycin C: Biological Effects and Use in Refractive Surgery. *Cornea* **2012**, *31*, 311-321.

29. Simman, R.; Alani, H.; Williams, F. Effect of Mitomycin C on Keloid Fibroblasts: An In Vitro Study. *Ann. Plast. Surg.* **2003**, *50*, 71-76.

30. Cupp, C.; Gaball, C. W. Utilizing Topical Therapies and Mitomycin to Reduce Scars. *Facial Plast. Surg.* **2012**, *28*, 513-517.

31. Ingrams, D. R.; Volk, M. S.; Biesman, B. S.; Pankratov, M. M.; Shapshay, S. M. Sinus Surgery: Does Mitomycin C Reduce Stenosis? *Laryngoscope* **1998**, *108*, 883-886.

32. Kumar, G. S.; Lipman, R.; Cummings, J.; Tomasz, M. Mitomycin C-DNA Adducts Generated by DT-Diaphorase. Revised Mechanism of the Enzymatic Reductive Activation of Mitomycin C. *Biochemistry* **1997**, *36*, 14128-14136.

33. Bargonetti, J.; Champeil, E.; Tomasz, M. Differential Toxicity of DNA Adducts of Mitomycin C. *J. Nucleic Acids* [Online] **2010**, Article 698960.

34. Chirrey, L.; Cummings, J.; Halbert, G. W.; Smyth, J. F. Conversion of mitomycin C to 2,7-diaminomitosene and 10-decarbamoyl 2,7-diaminomitosene in tumour tissue in vivo. *Cancer Chemother. Pharmacol.* **1995**, *35*, 318-322.

35. Warren, A. J.; Maccubbin, A. E.; Hamilton, J. W. Detection of Mitomycin C-DNA Adducts *in Vivo* by ^{32}P-Postlabeling: Time Course for Formation and Removal of Adducts and Biochemical Modulation. *Cancer Res.* **1998**, *58*, 453-461.

36. Warren, A. J.; Mustra, D. J.; Hamilton, J. W. Detection of Mitomycin C-DNA Adducts in Human Breast Cancer Cells Grown in Culture, as Xenografted Tumors in Nude Mice, and in Biopsies of Human Breast Cancer Patient Tumors as Determined by ^{32}P-Postlabeling. *Clin. Cancer Res.* **2001**, *7*, 1033-1042.

37. Paz, M. M.; Ladwa, S.; Champeil, E.; Liu, Y.; Rockwell, S.; Boamah, E. K.; Bargonetti, J.; Callahan, J.; Roach, J.; Tomasz, M. Mapping DNA Adducts of Mitomycin C and Decarbamoyl Mitomycin C in Cell Lines Using Liquid Chromtography/Electrospray Tandem Mass Spectrometry. *Chem. Res. Toxicol.* **2008**, *21*, 2370-2378.

38. Palom, Y.; Belcourt, M. F.; Musser, S. M.; Sartorelli, A. C.; Rockwell, S.; Tomasz, M. Structure of Adduct X, the Last Unknown of the Six Major DNA Adducts of Mitomycin C Formed in EMT6 Mouse Mammary Tumor Cells. *Chem. Res. Toxicol.* **2000**, *13*, 479-488.

39. Schwartz, H. S. Pharmacology of Mitomycin C: III. *In vitro* metabolism by rat liver. *J. Pharmacol. Exp. Ther.* **1962**, *136*, 250-258.

40. Hoey, B. M.; Butler, J.; Swallow, A. J. Reductive Activation of Mitomycin C. *Biochemistry*, **1988**, *27*, 2608-2614.

41. Paz, M. M. Reductive Activation of Mitomycin C by Thiols: Kinetics, Mechanism, and Biological Implications. *Chem. Res. Toxicol.* **2009**, *22*, 1663-1668.

42. Tomasz, M.; Lipman, R. Alklation Reactions of Mitomycin C at Acid pH. *J. Am. Chem. Soc.* **1979**, *101*, 6063-6067.

43. Siegel, D.; Gibson, N. W.; Preusch, P. C.; Ross, D. Metabolism of Mitomycin C by DT-Diaphorase: Role in Mitomycin C-induced DNA Damage and Cytotoxicity in Human Colon Carcinoma Cells. *Cancer Res.* **1990**, *50*, 7483-7489.

44. Pan, S.-S.; Andrews, P. A.; Glover, C. J.; Bachur, N. R. Reductive Activation of Mitomycin C and Mitomycin C Metabolites Catalyzed by NADPH-Cytochrome P-450 Reductase and Xanthine Oxidase. *J. Biol. Chem.* **1984**, *259*, 959-966.

45. Hodnick, W. F.; Sartorelli, A. C. Reductive Activation of Mitomycin C by NADH:Cytochrome b5 Reductase. *Cancer Res.* **1993**, *53*, 4907-4912.

46. Lown, J. W. The mechanism of action of quinone antibiotics. *Mol. Cell. Biochem.* **1983**, *55*, 17-40.

47. Valko, M.; Leibfritz, D.; Moncol, J.; Cronin, M. T. D.; Mazur, M.; Telser, J. Free radicals and antioxidants in normal physiological functions and human disease. *Int. J. Biochem. Cell Biol.* **2007**, *39*, 44-84.

48. Klaunig, J. E.; Kamendulis, L. M. The Role of Oxidative Stress in Carcinogenesis. *Annu. Rev. Pharmacol. Toxicol.* **2004**, *44*, 239-267.

49. Nordberg, J.; Arnér, E. S. J. Reactive Oxygen Species, Antioxidants, and the Mammalian Thioredoxin System. *Free Radical Biol. Med.* **2001**, *31*, 1287-1312.

50. Lown, J. W.; Begleiter, A.; Johnson, D.; Morgan, A. R. Studies related to antitumor antibiotics. Part V. Reactions of mitomycin C with DNA examined by ethidium fluorescence assay. *Can J. Biochem.* **1976**, *54*, 110-119.

51. Hamana, K.; Kawada, K.; Sugioka, K.; Nakano, M.; Tero-Kubota, S.; Ikegami, Y. DNA Strand Scission by Enzymatically Reduced Mitomycin C: Evidence for Participation of the Hydroxyl Radical in the DNA Damage. *Biochem. Int.* **1985**, *10*, 301-309.

52. Handa, K.; Sato, S. Generation of Free Radicals of Quinone Group-Containing Anti-Cancer Chemicals in NADPH-Microsome System as Evidence by Initiation of Sulfite Oxidation. *Gann* **1975**, *66*, 43-47.

53. Tomasz, M. H_2O_2 Generation during the Redox Cycle of Mitomycin C and DNA-bound Mitomycin C. *Chem.-Biol. Interact.* **1976**, *13*, 89-97.

54. Lown, J. W.; Sim, S.-K.; Chen, H.-H. Hydroxyl radical production by free and DNA-bound aminoquinone antibiotics and its role in DNA degradation. Electron spin resonance detection of hydroxyl radicals by spin trapping. *Can. J. Biochem.* **1978**, *56*, 1042-1047.

55. Komiyama, T.; Kikuchi, T.; Sugiura, Y. Generation of Hydroxyl Radical by Anticancer Quinone Drugs, Carbazilquinone, Mitomycin C, Aclacinomycin A and Adriamycin, in the Presence of NADPH-cytochrome P-450 Reductase. *Biochemical Pharmacology* **1982**, *31*, 3651-3656.

56. Bachur, N. R.; Gordon, S. L.; Gee, M. V. A General Mechanism for Microsomal Activation of Quinone Anticancer Agents to Free Radicals. *Cancer Res.* **1978**, *38*, 1745-1750.

57. Bachur, N. R.; Gordon, S. L.; Gee, M. V.; Kon, H. NADPH cytochrome *P*-450 reductase activation of quinone anticancer agents to free radicals. *Proc. Natl. Acad. Sci.* **1979**, *76*, 954-957.

58. Doroshow, J. H. Mitomcyin C-Enhanced Superoxide and Hydrogen Peroxide Formation in Rat Heart. *J. Pharmacol. Exp. Ther.* **1981**, *218*, 206-211.

59. Pritsos, C. A.; Sartorelli, A. C. Generation of Reactive Oxygen Radicals through Bioactivation of Mitomycin Antibiotics. *Cancer Res.* **1986**, *46*, 3528-3532.

60. Dusre, L.; Covey, J. M.; Collins, C.; Sinha, B. K. DNA Damage, Cytotoxicity and Free Radical Formation by Mitomycin C in Human Cells. *Chem.-Biol. Interact.* **1989**, *71*, 63-78.

61. Rockwell, S.; Kennedy, K. A.; Sartorelli, A. C. Mitomycin-C as a Prototype Bioreductive Alkylating Agent: In Vitro Studies of Metabolism and Cytotoxicity. *Int. J. Radiat. Onc., Biol., Phys.* **1982**, *8*, 753-755.

62. Keyes, S. R.; Rockwell, S.; Sartorelli, A. C. Porfiromycin as a Bioreductive Alkylating Agent with Selective Toxicity to Hypoxic EMT6 Tumor Cells *in Vivo* and *in Vitro*. *Cancer Res.* **1985**, *45*, 3642-3645.

63. Keyes, S. R.; Loomis, R.; DiGiovanna, M. P.; Pritsos, C. A.; Rockwell, S.; Sartorelli, A. C. Cytotoxicity and DNA Crosslinks Produced by Mitomycin Analogs in Aerobic and Hypoxic EMT6 Cells. *Cancer Commun.* **1991**, *3*, 351-356.

64. August, P. R.; Flickinger, M. C.; Sherman, D. H. Cloning and analysis of a locus (mcr) involved in mitomycin C resistance in Streptomyces lavendulae. *J. Bacteriol.* **1994**, *176*, 4448-4454.

65. Belcourt, M. F.; Penketh, P. G.; Hodnick, W. F.; Johnson, D. A.; Sherman, D. H.; Rockwell, S.; Sartorelli, A. C. Mitomycin resistance in mammalian cells expressing the bacterial mitomycin C resistance protein MCRA. *Proc. Natl. Acad. Sci. U.S.A.* **1999**, *96*, 10489-10494.

66. Mikami, K.; Naito, M.; Tomida, A,; Yamada, M.; Sirakusa, T.; Tsuruo, T. DT-Diaphorase as a Critical Determinant of Sensitivity to Mitomycin C in Human Colon and Gastric Carcinoma Cell Lines. *Cancer Res.* **1996**, *56*, 2823-2826.

67. Sagara, N.; Katoh, M. Mitomycin C Resistance Induced by *TCF-3* Overexpression in Gastric Cancer Cell Line MKN28 Is Associated with DT-diaphorase Down-Regulation. *Cancer Res.* **2000**, *60*, 5959-5962.

68. Baumann, R. P.; Hodnick, W. F.; Seow, H. A.; Belcourt, M. F.; Rockwell, S.; Sherman, D. H.; Sartorelli, A. C. Reversal of Mitomycin C Resistance by Overexpression of Bioreductive Enzymes in Chinese Hamster Ovary Cells. *Cancer Res.* **2001**, *61*, 7770-7776.

69. Wu, H. I.; Brown, J. A.; Dorie, M. J.; Lazzeroni, L.; Brown, J. M. Genome-Wide Identification of Genes Conferring Resistance to the Anticancer Agents Cisplatin, Oxaliplatin, and Mitomycin C. *Cancer Res.* **2004**, *64*, 3940-3948.

70. Danishefsky, S. J.; Egbertson, M. On the Characterization of Intermediates in the Mitomycin Activation Cascade: A Practical Synthesis of an Aziridinomitosene. *J. Am. Chem. Soc.* **1986**, *108*, 4648-4650.

71. Han, I.; Kohn, H. 7-Aminoaziridinomitosenes: Synthesis, Structure, and Chemistry. *J. Org. Chem.* **1991**, *56*, 4648-4653.

72. Kinoshita, S.; Uzu, K.; Nakano, K.; Shimizu, M.; Takahashi, T. Mitomycin Derivatives. 1. Preparation of Mitosane and Mitosene Compounds and Their Biological Activities. *J. Med. Chem.* **1971**, *14*, 103-109.

73. Hodges, J. C.; Remers, W. A. Synthesis and Antineoplastic Activity of Mitosene Analogues of the Mitomycins. *J. Med. Chem.* **1981**, *24*, 1184-1191.

74. Iyengar, B. S.; Remers, W. A.; Bradner, W. T. Preparation and Antitumor Activity of 7-Substituted 1,2-Aziridinomitosenes. *J. Med. Chem.* **1986**, *29*, 1864-1868.

75. Teng, S. P.; Woodson, S. A.; Crothers, D. M. DNA Sequence Specificity of Mitomycin Cross-Linking. *Biochemistry* **1989**, *28*, 3901-3907.

76. Li, V.-S.; Choi, D.; Tang, M.-S.; Kohn, H. Concerning *in Vitro* Mitomycin-DNA Alkylation. *J. Am. Chem. Soc.* **1996**, *118*, 3765-3766.

77. Vedejs, E.; Klapars, E.; Naidu, B. N.; Piotrowski, D. W.; Tucci, F. C. Enantiocontrolled Synthesis of (1*S*,2*S*)-6-Desmethyl-(methylaziridino)mitosene. *J. Am. Chem. Soc.* **2000**, *122*, 5401-5402.

78. Vedejs, E.; Naidu, B. N.; Klapars, A.; Warner, D. L.; Li, V.-s.; Na, Y.; Kohn, H. Synthetic Enantiopure Aziridinomitosenes: Preparation, Reactivity, and DNA Alkylation Studies. *J. Am. Chem. Soc.* **2003**, *125*, 15796-15806.

79. Rink, S. M.; Warner, D. L.; Klapars, A.; Vedejs, E. Sequence-Specific DNA Interstrand Cross-Linking by an Aziridinomitosene in the *Absence* of Exogenous Reductant. *Biochemistry*, **2005**, *44*, 13981-13986.

80. Wang, Z.; Jimenez, L. S. Synthesis of an Aziridinomitosene Analog. *J. Org. Chem.* **1996**, *61*, 816-818.

81. Dong, W.; Jimenez, L. S. Synthesis of a Fully Functionalized 7-Methoxyazridinomitosene. *J. Org. Chem.* **1999**, *64*, 2520-2523.

82. Michael, J. P.; de Koning, C. B.; Petersen, R. L.; Stanbury, T. V. Asymmetric synthesis of a tetracyclic model for the aziridinomitosenes. *Tetrahedron Lett.* **2001**, *42*, 7513-7516.

83. Wiedner, S. D.; Vedejs, E. Reactivity of Aziridinomitosene Derivatives Related to FK317 in the Presence of Protic Nucleophiles. *J. Org. Chem.* **2012**, *77*, 1045-1055.

84. Bonham, S.; O'Donovan, L.; Carty, M. P.; Aldabbagh, F. First synthesis of an aziridinyl fused pyrrolo[1,2-*a*]benzimidazole and toxicity evaluation towards normal and breast cancer cell lines. *Org. Biomol. Chem.* **2011**, *9*, 6700-6706.

85. Kunz, K. R.; Iyengar, B. S.; Dorr, R. T.; Alberts, D. S.; Remers, W. A. Structure-Activity Relationships for Mitomycin C and Mitomycin A Analogues. *J. Med. Chem.* **1991**, *34*, 2281-2286.

CHAPTER TWO: MECHANISMS OF AZIRIDINOMITOSENE CYTOTOXICITY

Two synthetic aziridinomitosenes (AZMs) were evaluated for their cytotoxicity in six human cancer cell lines, and the cellular effects compared to mitomycin C (MC). Me/H-AZM was found to be a more potent cytotoxic agent than either H/H-AZM or MC. H/H-AZM was the least cytotoxic of the three drugs, although it displayed increased potency over MC in the T47D cell lines. Several cellular effects of AZM and MC treatment were investigated in Jurkat and HeLa cell lines. Treatment with either AZMs increased intracellular oxidative stress relative to MC treatment, with H/H-AZM showing the greatest overall increase. Pre-treatment of Jurkat cell cultures with the antioxidant N-acetyl-L-cysteine (NAC) resulted in a measurable decrease of H/H-AZM cytotoxicity and no measurable changes in Me/H-AZM or MC cytotoxicity, suggesting that under the conditions tested H/H-AZM may work through increasing oxidative stress, while the primary cytotoxic effect of MC and Me/H-AZM was probably not mediated through increased oxidant stress. In HeLa cells, pretreatment with NAC produced a measurable increase in Me/H-AZM with no alterations observed in MC treatments. However, treatment of Jurkat or HeLa cell lines with any of the three drugs did produce a collapse in the mitochondrial membrane potential, with Me/H-AZM inducing the largest disruption. Apoptotic cell death was evaluated by measuring drug induced activation of caspase-3, by H/H-AZM, Me/H-AZM, or MC. In Jurkat cells, all three drugs were active, with MC treatment causing the largest activation of caspase-3. In HeLa cells, only MC treatments led to significant caspase-3 activation. Fluorescence microscopy of

MC, H/H-AZM, and Me/H-AZM treated cells showed the drugs also produced changes in nuclear morphology. All three drugs produced increased nuclear size in HeLa cells in at least one of the tested drug concentrations that were consistent with stimulating a necrotic, rather than apoptotic response. The results of these studies indicate that AZMs and MC share similarities in their cellular effects including the induction of mitochondrial membrane changes, activation of caspase-3, and stimulation of nuclear swelling. Furthermore, the two AZMs investigated display increased toxicity towards suspension cells over that of adherent cell lines, as well as increases in caspase-3 activity and more consistent oxidative stress.

Introduction

Aziridinomitosenes (AZMs) are organic compounds structurally related to the mitomycin family of chemotherapeutic agents. The original synthesis and characterization of AZMs was accomplished through reduction-oxidation reactions of mitomycin B (MB) and N-methyl mitomycin A (NMA).[1] As such, AZMs possess similar structural features including the presence of a tetracyclic core featuring an aziridine ring. The key distinction occurs with the departure of the functional group from carbon 9a and deprotonation at C9, leaving a double bond between carbons 9 and 9a in AZMs (Figure 2.1).[2-4]

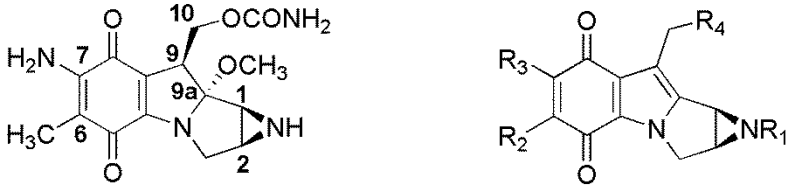

Mitomycin C Aziridinomitosene

Figure 2.1 Structures of Mitomycin C and a generic AZM. Partial carbon numbering scheme is displayed on MC and is consistent with the AZM architecture.

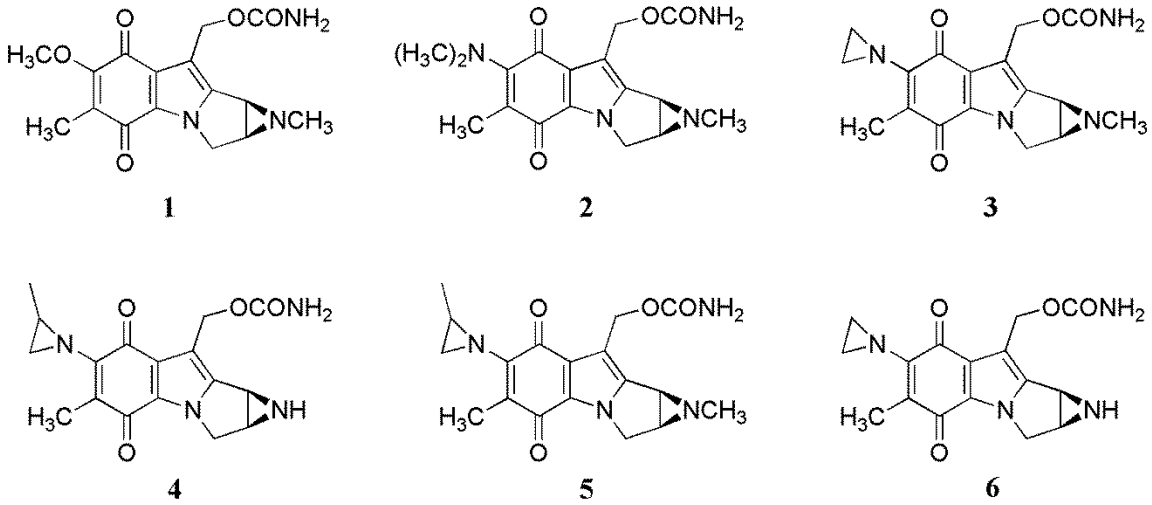

Figure 2.2 AZMs with appreciable biological activity. Structural depiction of some AZMs investigated that exhibit biological activity.[5-7]

Early investigations into the biological properties of AZMs were conducted primarily through the conversion from a corresponding mitomycin, followed by alterations to the C7 functional group or methylation of the aziridine nitrogen (Figure 2.2).[1,5-7] Of several AZMs, **1** was found to display similar properties to mitomycins, including broad spectrum bactericidal action and anti-tumor properties.[1,5] Antimicrobial activity against gram positive bacteria was shown by **2**, but it had limited effects on gram negative bacteria.[5] Similar activity to mitomycins was observed in **4** and **5**, but their measured responses required much larger dosages than MC. Similarly, while AZM **6** was more effective than MC at increasing the life span of mice inoculated with P-388 leukemia, the required AZM dose was higher than MC.[7] Despite these investigations into the biological and biochemical activity of AZMs, detailed description of the effects of AZM treatment on mammalian cells has not been published. A handful of studies have found AZMs capable of inducing DNA interstrand cross-linking (ICL) *in vitro* utilizing purified nucleic acids or oligonucleotides.[8-11]

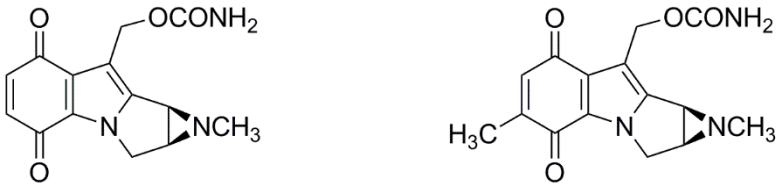

Figure 2.3 Structures of synthetic AZMs investigated in this study. H/H-AZM = (1S, 2S)-6-desmethyl(methylaziridino)mitosane, Me/H-AZM = (1S, 2S)-6-methyl(methylaziridino)mitosane.

In this study, we report the evaluation of cellular toxicity of two AZMs synthesized in our laboratory (1S, 2S)-6-desmethyl(methylaziridino)mitosane (H/H-AZM) and (1S, 2S)-6-methyl(methylaziridino)mitosane (Me/H-AZM) (Figure 2.3) against a small panel of six human cancer cell lines.[10] Cellular responses caused by AZM treatment in Jurkat and HeLa cell lines were explored to gain better insight into potential mechanisms of drugs action. Due to the structural similarities of AZMs and MC, we hypothesized that many of the characteristics of aziridinomitosene biological activity will parallel that of MC. Our approach was to measure several potential pathways that may contribute to drug cytotoxicity, including stimulation of oxidative stress, alterations to the mitochondrial membrane potential ($\Delta\Psi_m$), caspase-3 activation, and changes in nuclear morphology that would suggest apoptotic or necrotic pathways of cell death.

A number of chemotherapeutic drugs, including MC, have been shown to lead to increases in oxidative stress of cells.[12-21] The formation of reactive oxygen species (ROS) occurs naturally in cells as a by-product of the partial reduction of oxygen during respiration.[12,22] Typically, levels of ROS are maintained in a homeostatic balance by interactions with cellular antioxidants (vitamin E, vitamin C, glutathione, coenzyme Q) or enzymatic degradation (superoxide dismutase, catalase, glutathione peroxidase).[12,23] Elevated ROS levels in the cell can exceed the reductive capacity of anti-oxidant systems,

leading to oxidative damage of important intracellular biomolecules such as lipids, proteins, and DNA. This increased oxidative damage can lead to mutations, cancer, and cell death.[22]

The preservation of an intact $\Delta\Psi_m$ is essential to cellular health and proper mitochondrial function. The $\Delta\Psi_m$ is involved in functions such as the production of ATP, formation of ROS, mitochondrial protein transfer, and mitochondrial calcium sequestration.[24,25] Furthermore, the collapse of $\Delta\Psi_m$ can lead to an apoptotic cellular death due to the release of several pro-apoptotic factors including cytochrome c and pro-caspase enzymes.[26-29]

Cells undergoing an apoptotic cellular death experience several distinct features including chromatin condensation, nuclear fragmentation, and formation of apoptotic bodies.[30,31] Condensation of the nucleus has been associated with an apoptotic cellular death, whereas nuclear swelling is attributed to a necrotic cell death.[30,32] Previously, incubations with MC for 24 hours lead to an increase in nuclear area, while decarbamoyl MC (DMC) stimulated a decrease in nuclear area, indicating variations in their cytotoxic pathways.[32]

Many chemotherapeutic drugs induce apoptosis through either the death-receptor-induced extrinsic pathway or mitochondria-apoptosome-mediated apoptotic intrinsic pathway. Both paths result in caspase activation.[33,34] In particular, caspase-3 is activated in both extrinsic and intrinsic pathways. As such, it presents as a plausible enzyme to investigate for preliminary insight into evaluation of the apoptotic versus necrotic cellular death caused by H/H-AZM and Me/H-AZM.

Materials and Methods

Materials

Mitomycin C, 2',7'-dichlorodihydrofluorescein diacetate (DCFDA), and 5,5',6,6'-tetrachloro-1,1',3,3'-tetraethylbenzimidazolocarbocyanine iodide (JC-1) were purchased from Cayman Chemical (Ann Arbor, MI). HyClone growth media and penicillin/streptomycin were obtained from Thermo Scientific (Waltham, MA). Fetal Bovine Serum (FBS) and N-acetyl-L-cysteine (NAC) were purchased from Fisher Scientific (Hampton, NH). Resazurin sodium salt was acquired from Acros Organics (Fairlawn, New Jersey). Carbonyl cyanide 3-chlorophenylhydrazone (CCCP), and anhydrous dimethyl sulfoxide (DMSO) were obtained from Sigma (St. Louis, MO). Hoechst 33342 stain and EnzChek Caspase 3 Assay Kit #2 were purchased from Invitrogen (Carlsbad, CA).

Cell Culture Methods and Drug Stocks

Six different human cell lines were used to evaluate the potency of the AZMs and MC. These include three suspension (Jurkat, HUT-78, HL-60) and three adherent cancer cell lines (HeLa, T47D, HepG2). The Jurkat (T lymphocyte) and HuT-78 (cutaneous T lymphocyte) cell lines were obtained as a generous gift from Dr. Denise Wingett, Boise State University. The T47D (ductal carcinoma) and HL-60 (acute promyeloblastic leukemia) cell lines were kindly provided by Dr. Cheryl Jorcyk, Boise State University. The HepG2 (hepatocellular carcinoma) cell line was a generous gift from Dr. Kristen Mitchell, Boise State University. Lastly, the HeLa (cervical adenocarcinoma) cell line were obtained generously from Dr. Ken Cornell, Boise State University.

Jurkat and T47D cells were cultured in RPM1-1640 supplemented with 10% FBS and penicillin (100 U/mL) and streptomycin (100 µg/mL) (pen/strep). HeLa and HepG2 cell lines were grown utilizing Dulbecco's Modified Eagles Medium (DMEM) containing 10% FBS with pen/strep. Finally, HL-60 and HUT-78 cell lines were cultured in Iscove's Modified Dulbecco's Medium (IMDM) supplemented with 20% FBS and pen/strep. All cell lines were grown at 37 ºC in 5% CO_2.

All three compounds (H/H-AZM, Me/H-AZM, and MC) were dissolved in DMSO to create concentrated drug stocks that were stored at -80 ºC prior to use. H/H-AZM and Me/H-AZM were synthesized in our laboratory according to previously reported methods.[10]

Resazurin Cytotoxicity Assay

Cells were seeded into a 96 well plate at a density of 8,000 cells/well and incubated at 37 ºC in 5% CO_2 overnight. For adherent cell lines, media was replaced with 180 µL of fresh media with 10% FBS and pen/strep, and 20 µL of 10x drug stock (diluted in nanopure H_2O) or 20 µL vehicle. Cultures were incubated with drug for 48 hours at 37 ºC in 5% CO_2. After 48 hours, 20 µL of 0.1% resazurin in 1x PBS was added to all wells (10% of the total well volume), and the culture incubated with dye for 4-24 hours to allow metabolic conversion of resazurin (blue) to resorufin (pink). Fluorescence values (excitation 530 ± 25 nm and emission 590 ± 35 nm) were then obtained using a BioTek Synergy HT plate reader (BioTek, Winooski, VT). Fluorescence data was plotted in GraphPad Prism using a non-linear regression with log (inhibitor) vs. response (three parameter) for determination of IC_{50} values. Data are represented as the mean ± SEM, for at least three experiments.

Reactive Oxygen Species Assay

The abcam "DCFDA-Cellular Reactive Oxygen Species Assay Kit (ab113851)" protocol was used with slight adaptations.[39] Jurkat cells were harvested via centrifugation at 150 x g for 5 minutes, and adjusted to a density of approximately 1 x 10^6 cells/mL, after washing once with Kreb's Ringer Bicarbonate (KRB) buffer, pH =7.4. Cells were stained with 20 µM DCFDA in KRB buffer for 30 minutes at 37 ºC. After 30 minutes, cells were harvested, washed once in KRB buffer, then resuspended in KRB + 10% FBS. Followed by an addition of 100 µL cell solution into a black 96 well plate and combined with 100 µL of 2x drug dilution (made in KRB + 10% FBS solution) or 100 µL KRB + 10% FBS solution. Fluorescence was immediately read on a Biotek Synergy HT plate reader (BioTek, Winooski, VT) using excitation 485 ± 20 and emission 528 ± 20 nm. Additional readings were then taken at three and six hours after addition of drug treatments. Data was worked up in Microsoft Excel and plotted in GraphPad Prism 6 as the mean ± SEM, for at least three experiments.

HeLa cells were seeded into a black 96 well plate at 2.5 x 10^4 cells/well and allowed to adhere overnight. Media was removed; the cells were washed once with KRB, and were stained with 20 µM DCFDA in Kreb's Ringer Bicarbonate Buffer for 30 minutes at 37 ºC. The staining solution was removed and the cells were washed twice in KRB Buffer and then suspended in KRB + 10% FBS. Buffer (100 µL) was added to all wells and combined with either, 100 µL of 2x drug dilution (made in KRB + 10% FBS solution) or 100 µL KRB + 10% FBS solution. Fluorescence was immediately read on a Biotek Synergy HT plate reader (BioTek, Winooski, VT) using excitation 485 ± 20 and emission 528 ± 20 nm. Additional readings were then taken at three and six hours post

drug treatments. Data was worked up in Microsoft Excel and plotted in GraphPad Prism 6 as the mean ± SEM, for at least three experiments.

N-acetyl-L-cysteine Cytotoxicity Assay

HeLa cells were seeded into a 96 well plate at a density of 8,000 cells/well and allowed to adhere overnight at 37 ºC in 5% CO_2. The next day, media was replaced with fresh 90% DMEM/10% FBS with pen/strep and cells were incubated with 5 mM N-acetyl-L-cysteine (NAC) in complete media for 15 minutes at 37 ºC in 5% CO_2. NAC containing media was removed, cells were washed twice with 1x PBS, and 180 µL of fresh 90% DMEM/10% FBS with pen/strep added to all wells. As presented above in "Resazurin Cytotoxicity Assay", the cells were then treated with MC, H/H-AZM, and Me/H-AZM for 48 hours. The cells were then treated with 20 µL of 0.1% Resazurin in 1x PBS to all wells and incubated for 4 hours at 37 ºC in 5% CO_2. Fluorescence was then measured on a Biotek Synergy HT plate reader using excitation 530 ± 25 nm and emission 590 ± 35 nm, with sensitivity set to 35. Data was then analyzed and worked up in Microsoft Excel and plotted in GraphPad Prism 6 as the mean ± SEM, for at least three experiments.

Jurkat cells were harvested via centrifugation at 150 x g for 5 minutes at 4 ºC, washed once with complete media, and then suspended in 90%RPMI-1640/10% FBS with pen/strep and 5 mM NAC. The Jurkat cells were allowed to incubate with the 5 mM NAC solution for one hour at 37 ºC in 5% CO_2, after which time they were harvested via centrifugation, washing twice in complete media.[29] The cells were then suspended in complete media and placed in a 96 well plate at a density of 8,000 cells/well at a final volume of 180 µL. Drug dilutions were then added to appropriate wells in pentet,

allowing for untreated controls, as well as cells that were not incubated with NAC solution. Cells were allowed to incubate with drug for 48 hours at 37 ºC in 5% CO_2. The cells were then treated with 20 µL of 0.1% resazurin in 1x PBS to all wells and incubated for 24 hours at 37 ºC in 5% CO_2. Fluorescence was then measured on a Biotek Synergy HT plate reader using excitation 530 ± 25 nm and emission 590 ± 35 nm, with sensitivity set to 35. Data was then analyzed and worked up in Microsoft Excel and plotted in GraphPad Prism 6 as the mean ± SEM, for at least three experiments.

Mitochondrial Membrane Potential Assay

Changes in the mitochondrial membrane potential were assessed using the JC-1 dye following a slight adaptation to the abcam "JC-1 Mitochondrial membrane potential Assay kit (ab113850)" protocol, in black clear bottom 96 well plates.[24] In cells with intact mitochondrial membrane potential the JC-1 dye fluoresces is unable to enter the mitochondria and present as aggregates that fluoresce red. Upon dissolution of membrane potential, JC-1 is able to enter the mitochondria as monomers (green), leading to a decrease in aggregate fluorescence. The alterations in aggregate fluorescence were utilized in this assay.

Briefly, Jurkat cells were harvested via centrifugation obtaining approximately 2.5 x 10^7 cells, then washing once with KRB buffer at pH =7.4. Cells were then stained with 1 µM JC-1 in KRB buffer in the dark for 30 minutes at 37 ºC in 5% CO_2. After 30 minutes, cells were harvested via centrifugation, washed once in KRB buffer, and suspended in 5 mL of KRB + 10% FBS. The cell solution was then seeded into a 96 well plate at volume of 50 µL/well and combined with 50 µL of 2x drug dilutions made in KRB + 10% FBS solution or 50 µL KRB + 10% FBS solution. The plate was allowed to

incubate in the dark for 2 hours at 37 ºC in 5% CO_2. The fluorescence was measured using a Biotek Synergy HT plate reader with excitation/emission of 530/590 nm and sensitivity of 70. Data was worked up in Microsoft Excel and plotted using GraphPad Prism 6 as the mean ± SEM, for at least three independent experiments.

HeLa cells were seeded into a 96 well plate at 6 x 10^3 cells/well and allowed to adhere overnight. Media was removed and cells were washed once with KRB buffer, followed by staining with 1 µM JC-1 dye in KRB buffer for 10 minutes at 37 ºC in 5% CO_2. After 10 minutes, staining solution was removed, cells were washed twice with KRB buffer, and 100 µL of KRB buffer + 10% FBS added to all wells. Treatments were added to appropriate wells as 100 µL of 2x drug dilution or 100 µL KRB + 10% FBS solution. The cells were allowed to incubate in the dark for two hours at 37 ºC in 5% CO_2. The fluorescence was measured using a Biotek Synergy HT plate reader with excitation/emission of 530/590 nm and sensitivity of 70. Data was worked up in Microsoft Excel and plotted using GraphPad Prism 6 as the mean ± SEM, for at least three experiments.

Caspase 3 Assay

Evaluations into caspase 3 activation were conducted using the Molecular Probes EnzChek Caspase 3 Assay Kit #2 following the manufacturer's instructions. Briefly, 1 x 10^6 Jurkat or HeLa cells were seeded into 12 well plates. Cells were then treated with IC_{50} concentrations of MC, H/H-AZM, and Me/H-AZM for 24 hours at 37ºC in 5% CO_2. Cells were then harvested and washed with 1x PBS via centrifugation at 150 x g for 5 minutes at 4ºC. From here the manufacturer's protocol was then followed. Plates were read on a Biotek Synergy HT plate reader using an excitation of 485 ± 20 nm and

emission of 528 ± 20 nm, every 5 minutes for one hour at a sensitivity of 50. Data was worked up in Microsoft Excel and plotted in GraphPad Prism 6.

Nuclear Morphology Assay

To investigate the effects of AZMs on nuclear morphology, HeLa cells were grown to approximately 75% confluency in sterile 24 well plates at 37ºC in 5% CO_2. Media was replaced with fresh complete media, and 10x drug dilutions in 1x PBS were added to appropriate wells. Cells were then incubated with drugs for 24 hours at 37°C in 5% CO_2. After 24 hours, cells were washed twice with 1x PBS, followed by fixation with 2% paraformaldehyde in 1x PBS for 10 minutes at room temperature. After formaldehyde fixation, cells were washed twice with 1x PBS, and permeabilized with 0.1% Triton X-100 in 1x PBS for 5 minutes at room temperature. Nuclei were then stained using 1.0 µg/mL Hoechst 33342 in nanopure H_2O for 15 minutes at room temperature. Cell nuclei were visualized and photographed on an AMG Evos fl microscope using the 40x objective with the DAPI filter. Nuclear areas were measured using NIH ImageJ and data worked up and plotted using GraphPad Prism 6 as the mean ± SEM of two experiments counting over 100 nuclei for each treatment.[32,47]

Results and Discussion

Resazurin Cell Viability Assay

The resazurin fluorescence assay is a convenient method to examine the effect of cytotoxic agents on cell viability and proliferation (Table 2.1, Figure 2.4).[35,36] The reduction of the blue non-fluorescent resazurin to the pink fluorescent resorufin occurs in healthy cells maintaining a reducing environment.[35] The results of anti-

proliferative/cytotoxic activity assays in six human cancer cell lines (3 adherent, 3 suspension) are summarized in Table 2.1. All three compounds (Me/H-AZM, H/H-AZM, MC) showed anti-proliferative effects against the six cancer cell lines that were examined, with drug IC_{50} values ranging from low nanomolar to low micromolar concentrations.

Me/H-AZM was identified as the most potent compound of the three. Me/H-AZM was most toxic in Jurkat cells with an IC_{50} value of 3.11 ± 0.57 nM and least toxic in HeLa cells (IC_{50} = 525 ± 242 nM). H/H-AZM was overall the least toxic of the three, except in T47D cells where it showed a lower IC_{50} value (9.3 µM) than MC (17 µM). In comparison to MC, Me/H-AZM was at least 2 fold more toxic in every cell line, while H/H-AZM was at least 2 fold less toxic in all cell lines except T47D and Jurkat.

Table 2.1 Summary of drug cytotoxicity. IC_{50} values are the mean ± SEM from three experiments.

	IC_{50} (nM)		
	Mitomycin C	**H/H-AZM**	**Me/H-AZM**
HeLa	1,870 ± 372	6,208 ± 523	525 ± 242
T47D	16,970 ± 1,472	9,291 ± 1,516	225 ± 78
HepG2	2,937 ± 209	7,870 ± 701	342 ± 73
HL-60	409.6 ± 85.5	2,033 ± 967	29.9 ± 4.8
Jurkat	261.8 ± 70.8	218.7 ± 50.9	3.11 ± 0.57
HuT-78	66.4 ± 33.0	131.2 ± 47.9	23.7 ± 16.5

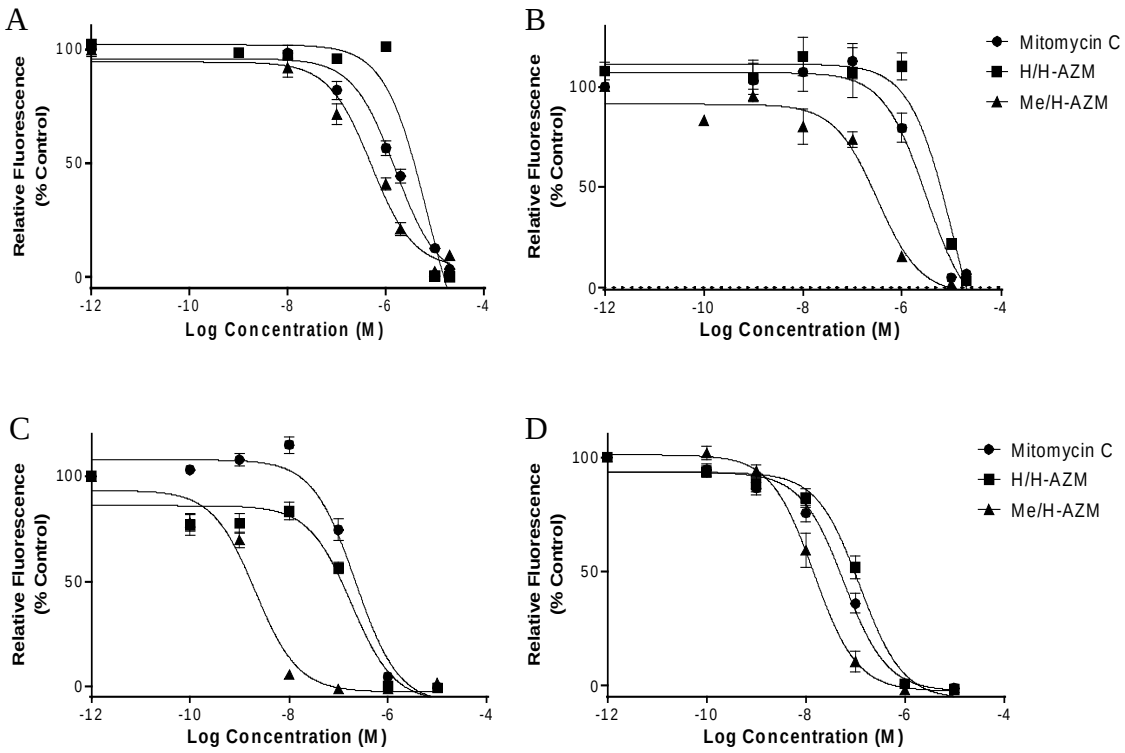

Figure 2.4 Antiproliferative activity of AZMs and MC. Representative results of investigating drug antiproliferative effects against four cell lines: A) HeLa, B) HepG2, C) Jurkat, and D) HuT-78. Relative fluorescence was calculated by dividing the average fluorescence of drug treated cells by the average untreated value, and multiplied by 100 to obtain a relative percent to untreated samples. Points represent the mean (± SEM) of three experiments.

The increased potency of Me/H-AZM may be due to preservation of the methyl group at C6, lack of a hydrophilic amine group at C7, and methylation of the aziridine ring (Figure 2.3) that may help to increase its lipophilicity and allow for more facile passage through membranes and into cells. In addition, the presence of an electron donating methyl group on the quinone ring may help to preserve the electrophilic integrity of the AZM, stabilizing the molecule for reactions with cellular nucleophiles. On the other hand, electron deficiencies at carbon 6 and 7 in H/H-AZM provide additional electrophilic sites that may be reactive and lead to reduced drug stability and lower activity *in vitro*. Nucleophilic addition at these locations shortly after introduction

into the cellular environment may hinder the cytotoxicity or allow it (H/H-AZM) to become sequestered by cellular nucleophiles prior to reaching a cellular target of significance.

Reactive Oxygen Species Assay

Due to the presence of a quinone moiety in the AZM structure, the potential for generation of ROS is highly plausible. Other quinone containing compounds, including the mitomycins have been found to increase levels of ROS.[12,14,15] MC itself has been shown to increase the production of hydrogen peroxide, superoxide anion, and hydroxyl radicals.[13-18,20] The cell permeable dye, 2'7'-dichlorofluoresceine diacetate (DCFDA), has been used as a probe to evaluate the level of oxidative stress within cells.[19] Previously, DCFDA has been used to examine changes in oxidative stress due to MC treatment of MCF-7 cells under both normoxia and hypoxia conditions.[21]

Using DCFDA as a probe, H/H-AZM treatment of both Jurkat and HeLa cell lines was found to increase ROS over 4-5 fold relative to untreated cells (Figure 2.5). Responses to Me/H-AZM varied depending on the cell line. In Jurkat cells, Me/H-AZM treatment stimulated a greater than 4 fold increase in ROS over untreated cells. Me/H-AZM treatment of HeLa cells stimulated a less drastic ROS response, with only a ~2 fold increase relative to untreated cells. In both cell lines, the measured oxidative stress attributed to MC treatment was essentially equivalent to the levels detected in untreated cells. Results from MC treatment appear to be consistent with the studies performed in MCF-7 breast cancer cells using DCFDA as the oxidative stress probe under normoxia.[21]

The additional electrophilic sites located at the C6/7 sites in H/H-AZM may allow for the reactions with intracellular antioxidants. H/H-AZM has been shown to react more

quickly than Me/H-AZM with thiols, such as glutathione (unpublished results). This interaction of H/H-AZM with thiols may lead to a reduction in intracellular glutathione levels, thus lowering the ability of the cell to combat oxidative stress. A similar but limited effect may be present in Me/H-AZM, as it also possesses an additional electrophilic site with a functional group vacancy at carbon 7. Me/H-AZM has also been shown to be reactive with thiols (unpublished results), which may explain the increased oxidative stress observed in Me/H-AZM treated cells.

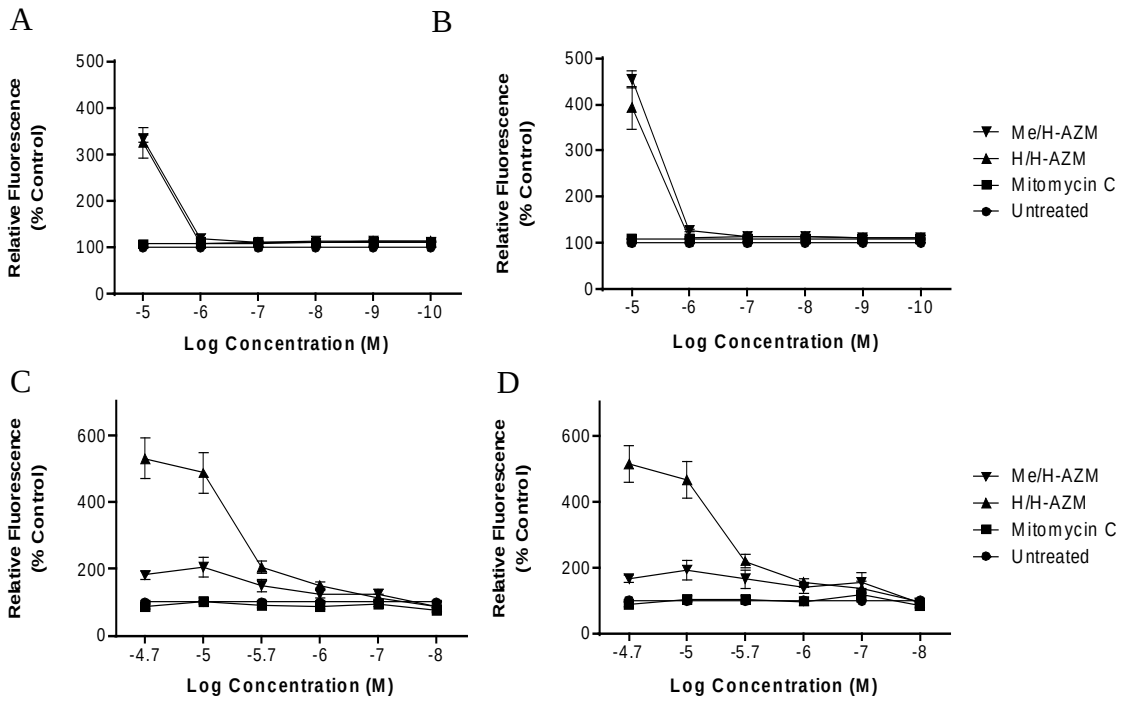

Figure 2.5 Oxidative stress responses in drug treated cells. Jurkat and HeLa cells were labeled with DCFDA for 30 minutes prior to addition of drug. Fluorescence measurements (ex 485 nm/em 528 nm) were made at 3 and 6 hours post drug addition. Relative fluorescence was calculated by dividing the average fluorescence of drug treated cells by the average untreated value, and multiplied by 100 to obtain a relative percent to untreated samples. Data shown is the mean ± SEM of three experiments (n = 9) A) Jurkat cells 3 hours post drug addition, B) Jurkat cells 6 hours post drug addition, C) HeLa cells 3 hours post drug addition, D) HeLa cells 6 hours post drug addition.

N-acetyl Cysteine Cytotoxicity Assay

N-acetyl-L-cysteine (NAC) is a precursor to glutathione, a cellular antioxidant used to combat ROS. Glutathione exists as the most prevalent low molecular weight thiol in mammalian cells. It is present in two forms GSH (reduced) or GSSG (oxidized), with the reduced form occurring at concentrations 10-100 fold higher than the oxidized form.[22,23] NAC protects against intracellular oxidative stress by scavenging radicals.[38,27] Pretreatment with 5 mM N-acetyl-L-cysteine was used to evaluate the relationship between oxidative stress and AZM induced cell death based on the premise if a major pathway to cytotoxicity is caused by increased oxidative stress, NAC should provide an additional antioxidant supply to combat the excess formation of free radicals, leading to decreased toxicity under AZM treatment.

Pretreatment with 5 mM NAC, Jurkat cells did not provide a protective effect against MC and Me-H/AZM treatments, with calculated IC_{50} values of the non-pretreated and NAC pretreated experiments falling within experimental errors of each other (Figure 6). H/H-AZM experiences a diminished cytotoxicity after pre-treatment with NAC. Based on the calculated IC_{50} values between the NAC pretreated groups and non-NAC pretreated groups, NAC exerts a protective effect upon H/H-AZM in Jurkat cells. Previous reports revealed a protective effect with NAC pre-treatment in epidural scar fibroblasts, with inhibition of MC induced apoptosis.[38]

In HeLa cells, results were inconsistent for H/H-AZM in both the presence and absence of NAC during this time and require further investigations. MC retained its cytotoxicity with IC_{50} values falling within experimental error of each other for the NAC pre-treated and cells, which were not pre-treated. Me/H-AZM toxicity appeared to

increase slightly with NAC pre-treatment, with a calculated IC_{50} 168.4 ± 27.8 nM. This increased toxicity may result from activation of the AZM through nucleophilic attack of the thiol at the C7 position. Previous studies have shown that mitomycin A (MA) and MC can undergo reductive activation with thiols including glutathione to form DNA cross-links.[40,41]

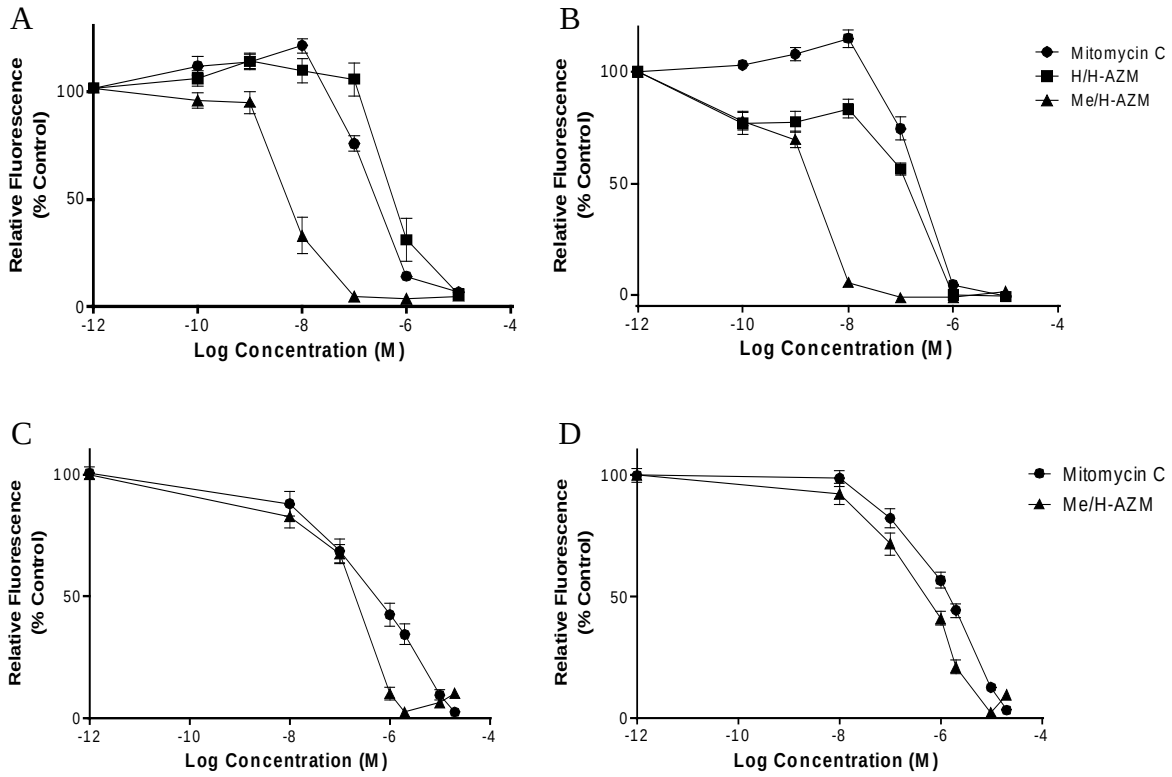

Figure 2.6 NAC pre-treatment and Resazurin Drug Treated Curves. Jurkat cells were either pretreated with 5 mM NAC for 1 hour + drug treatment (A), or drug treated (B). HeLa cells were either pretreated with 5 mM NAC for 15 minutes + drug treatment (C), or drug treated (D), H/H-AZM not shown as results were inconsistent. Cells in fresh media were then seeded into a 96-well plate at 8,000 cells/well and treated with drug for 48 hours. After 48 hours, 20 µL of 0.1% resazurin in 1x PBS was added to all wells. Cells were allowed to incubate with resazurin solution for 4-24 hours. Plates were then read using an excitation 530 ± 25 nm and emission 590 ± 35 nm. Data is a representation of the mean ± SEM of three experiments, n = 5, 1 x 10^{-12} M was considered the concentration at which there was not a drug effect for the untreated controls.

Mitochondrial Membrane Potential Assay

A breakdown in the ability to maintain the mitochondrial membrane potential can lead to excess production and leakage of ROS into the cytoplasm. Due to the increased levels of oxidative stress caused by H/H-AZM and Me/H-AZM, as measured by the DCFDA assay, a disruption of $\Delta\Psi_m$ would likely be the greatest in AZM treated samples. An alteration in the $\Delta\Psi_m$ of Jurkat and HeLa cells were found to occur after two hours with MC, H/H-AZM, and Me/H-AZM treatments (Figure 2.7). This was observed through the fluorescence decrease in aggregates of the cationic, lipophilic JC-1 dye. MC has been previously shown to lead to changes in $\Delta\Psi_m$ in corneal endothelial cells after 24 hour treatment.[42]

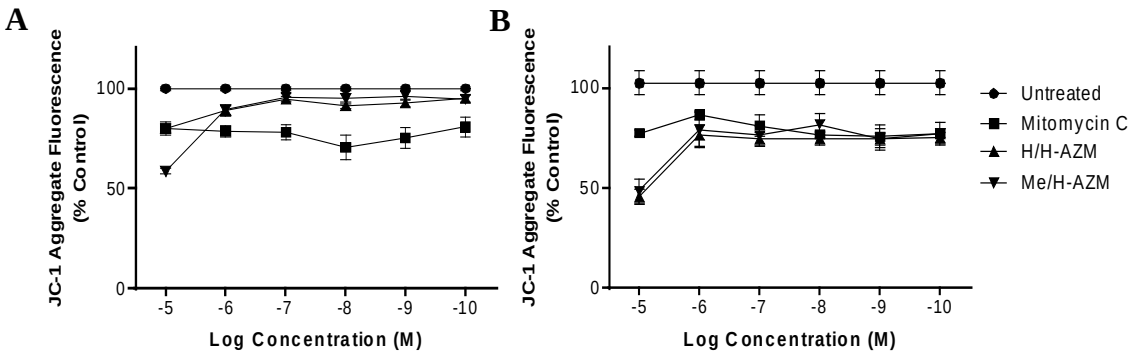

Figure 2.7 Mitochondrial Membrane Potential. A) Jurkat and B) HeLa cells were incubated with 1 µM JC-1 in KRB buffer for 30 or 10 minutes respectively, at 37ºC in %5 CO_2. JC-1 aggregate fluorescence was then read at 2 hours post drug addition using ex/em of 530/590 nm and plate reader sensitivity of 50. Plates were incubated at 37ºC in %5 CO_2 in the dark between readings. A) Jurkat cells; B) HeLa cells. Data shown is the mean ± S.E.M of three experiments, n = 9.

At lower concentrations, H/H-AZM treated aggregate fluorescence remained fairly constant, at around 70% of the untreated HeLa cells. MC treatments led to decreases in JC-1 aggregate fluorescence in each cell line, remaining fairly constant at each concentration. Previous studies in other cell lines have shown that MC treatment

leads to changes in the $\Delta\Psi_m$, and this result is consistent with our MC investigations in the Jurkat and HeLa cell lines.[42]

Me/H-AZM was the most effective in altering JC-1 aggregation as indicated by the decrease in fluorescence to about 50% of the untreated controls in both cell lines. H/H-AZM presented with similar decreases to MC in Jurkat cell lines, decreasing aggregate fluorescence to approximately 80% of the untreated control. In HeLa cells, H/H-AZM decreased JC-1 aggregate fluorescence similar to Me/H-AZM, around 50% of untreated cells at higher concentrations.

Both AZMs lead to a decrease in JC-1 aggregate fluorescence in each cell line. This result is consistent with our expectation that due to the increased levels of oxidative stress measured in the DCFDA assay, it is likely there will be alterations to the mitochondrial membrane potential. It is unclear if the mitochondria is a direct target of AZMs but evidence supports that this organelle is affected by treatment with these compounds.

Caspase 3 Activation

Caspase-3 is a downstream effector caspase activated through two pathways in apoptotic cell death. MC induced activation of caspases has been documented previously, including the stimulation of caspase-3.[43-45] After 24 hours of incubation, all compounds were found to activate caspase-3 more than the untreated controls in the Jurkat cell lines (Figure 2.8). MC (262 nM) had the most substantial effect, followed by H/H-AZM (220 nM), while Me/H-AZM (3 nM) produced the lowest levels of caspase-3 activation of the three compounds. In the HeLa cell line, MC (1.87 μM) was the only drug that significantly activated caspase-3 over that of the untreated sample. Treatments

with H/H-AZM (6.2 μM) and Me/H-AZM (525 nM) led to caspase-3 activity similar to that observed in the untreated samples.

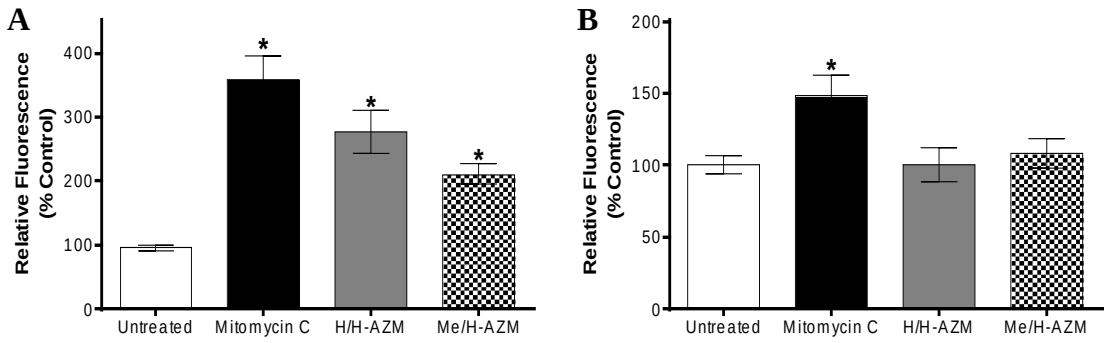

Figure 2.8 Caspase 3 activation by 24 hour treatment. A) Jurkat and B) HeLa cells were treated with IC_{50} concentrations of drug for 24 hours. Cells were then subject to the protocol outlined in materials and methods. Data is presented as the mean ± SEM of three experiments, n = 18 for Jurkat cells, n = 9 for HeLa cells. * denotes $p < 0.05$ as determined by one-way ANOVA when compared to untreated sample.

Activation of caspase-3 is consistent with forms of apoptotic cell death. The increased levels of caspase-3 displayed in treatments with MC, H/H-AZM, and Me/H-AZM signify a likelihood of apoptotic cell death, rather than necrosis. Since caspase-3 is an effector caspase activated via both apoptotic pathways, further inquiry into which of the initiator caspases become activated with AZM treatment is needed in order to develop a clear understanding of whether AZM induced apoptosis follows the death-receptor-induced extrinsic or mitochondria-apoptosome-mediated apoptotic intrinsic pathway.[33,34]

Nuclear Morphology Assay

Apoptotic cells undergo fragmentation of chromosomes, leading to condensation of the nucleus. During necrotic cell death, nuclei experience swelling as the cell loses its membrane integrity and is no longer able to regulate its osmotic balance.[30,46] Nuclear swelling as a result of 10 μM MC has been observed previously in cells treated for 24

hours. In the same study, the decarbamoyl MC derivative (DMC) was found to lead to nuclear condensation with the same dosage.[32] In this study, HeLa nuclear areas were assessed using the DNA fluorescent stain Hoechst 33342 and NIH ImageJ after 24 hour treatment (Figure 2.9).[32,32]

Treatment with 10 μM H/H-AZM and MC lead to a significant increase in HeLa nuclear area when compared to the untreated control. After 24-hour treatment with 10 μM Me/H-AZM, a majority of the HeLa cells became detached from the plate making it difficult to find remaining nuclei. The measurable nuclei were found to be significantly condensed when compared to the untreated samples, likely attributed to cell death. However, nuclear swelling followed by cell death could have occurred well before the 24 hour measurement, which would mean that the event was missed prior to measuring nuclear area. With 1 μM treatments, both MC and Me/H-AZM produced nuclear swelling, while H/H-AZM treated nuclei were, on average, more condensed than the untreated control. A similar pattern was observed in the 100 nM treatment groups, with MC and Me/H-AZM causing nuclear swelling, with no effect observed in the H/H-AZM treated cells. At 10 nM, there was no observable drug treated effect as nuclear areas were consistent with the untreated control. The alterations in the nuclear morphology imply that MC and Me/H-AZM may induce a similar mechanism of cell death with observed nuclear swelling at 1 μM and 100 nM concentrations. Of particular curiosity was the nuclear condensation witnessed in HeLa cells treated with 1 μM H/H-AZM, after observed swelling in the 10 μM treatments. An observed increase in nuclear area displayed by both AZMs and MC implies that they follow a similar mechanism of action in HeLa cells.

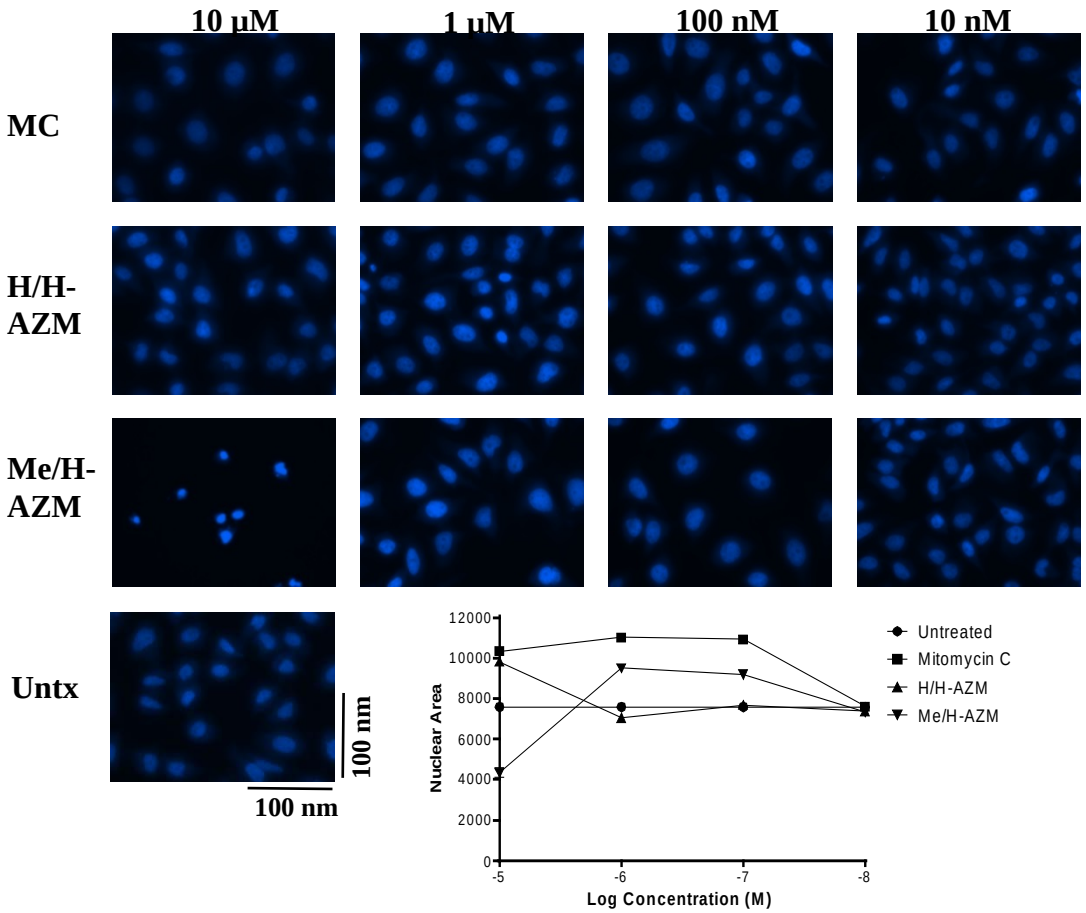

Figure 2.9 HeLa Cell Nuclear Morphology and Area. HeLa cells were grown to approximately 75% confluency in 24 well plates at 37 ºC in 5% CO_2. They were then either left untreated, or treated with MC, H/H-AZM, or Me/H-AZM for 24 hours. The cells were fixed in 2% paraformaldehyde, permeabilized using 0.1% Triton X-100, then stained with 1.0 µg/mL Hoechst 33342. Cell nuclei were then visualized on an AMG Evos fl microscope using the 40x objective and DAPI filter. Nuclear areas were measured using NIH ImageJ. Data is presented as the mean ± SEM from two experiments, n > 100 for each treatment. * denotes $p < 0.05$ as determined by one-way ANOVA when compared to untreated sample.

Conclusion

A widespread approach in determining the characteristics of two synthetic AZMs and their associated cytotoxicity was conducted. Our initial hypothesis was that AZM induced cellular death follows a similar pathway to MC and there appear to be some parallels in the cellular effects caused by treatment with MC and AZMs. Evaluations into

the potency of AZMs and MC were determined using a resazurin reduction assay to obtain an IC_{50} value in six different human cancer cell lines.[35,36] Me/H-AZM was more efficacious in decreasing cell viability when compared to both H/H-AZM and MC across all cell lines. The most drastic difference in drug toxicity was observed in T47D cells, where Me/H-AZM was 74 fold more potent than MC. In contrast, H/H-AZM was the least effective compound in decreasing cell viability, with increased potency compared to MC in only the T47D cell line.

Jurkat and HeLa cells treated with AZMs lead to increased production of ROS, when compared to the untreated controls. MC induced levels of ROS, remained consistent with the untreated sample in each cell line, correlating well with a study in MCF-7 cells utilizing DCFDA.[21] To evaluate whether this increased ROS production was a major factor in the AZM induced cell death, we employed pre-treatment with the oxygen radical scavenger, NAC. Pre-treatment with NAC did not produce a significant decrease in Me/H-AZM or MC associated cytotoxicity in Jurkat cells. However, NAC pretreatment produced a protective effect against H/H-AZM treatments in Jurkat cells. In HeLa cells, NAC pre-treatment stimulated Me/H-AZM toxicity with a drop in the calculated IC_{50} value, but remained the same in MC. Results from H/H-AZM in HeLa cells were inconsistent and require further investigation. These results indicate that a protective effect by NAC was observed in Jurkat cells treated with H/H-AZM, but not MC and Me/H-AZM. Similar results were seen in HeLa cells with MC and Me/H-AZM treatments. No conclusions can be drawn regarding H/H-AZM and NAC pre-treatment in HeLa cells.

Collapse of the mitochondrial membrane potential is affiliated with an apoptotic cell death with the release of pro-caspases and cytochrome c.[25] In addition, disruption of the $\Delta\Psi_m$ can lead to increased levels of ROS. As a consequence to the increased ROS production measured by AZM treatments, attention was directed towards measuring a potential collapse in $\Delta\Psi_m$. After two hours, a change in the $\Delta\Psi_m$ was observed by treatments with all three compounds in both cell lines, with Me/H-AZM leading to the largest decrease in aggregate fluorescence. H/H-AZM treatment lead to a greater disruption of $\Delta\Psi_m$ in HeLa over Jurkat cells.

The activation of caspase 3 occurs in the death-receptor-induced extrinsic pathway or mitochondria-apoptosome-mediated apoptotic intrinsic pathway.[33] Previous studies have shown that MC treatment leads to activation of caspase 3.[38,42-45] Treatment with IC_{50} concentrations lead to a significant increase in caspase 3 activity with all three drugs in Jurkat cells. MC led to the largest increase in caspase 3 activity, followed by H/H-AZM and Me/H-AZM. However, in HeLa cells only MC was shown to produce a significant increase in caspase-3 activity over that of the untreated controls.

Our initial hypothesis that AZMs follow a similar pattern as MC in their cellular effects appeared to be moderately correct. Similarities in their cellular effects include alterations in $\Delta\Psi_m$, caspase-3 activation, nuclear swelling by each drug in at least one drug concentration, and continuity of cytotoxicity after NAC pre-treatment (in Jurkat cells). Deviations in AZM and MC cellular effects were observed in AZM increased oxidative stress, while not measured in MC treatments. While there are some shared cellular effects between MC, H/H-AZM, and Me/H-AZM, there is much more work to be done in characterizing the many effects AZMs have in cellular treatments.

References

1. Patrick, J. B.; Williams, R. P.; Meyer, W. E.; Fulmor, W.; Cosulich, D. B.; Broshard, R. W.; Webb, J. S. Aziridinomitosenes: A New Class of Antibiotics Related to the Mitomycins. *J. Am. Chem. Soc.* **1964**, *86*, 1889-1890.
2. Webb, J. S.; Cosulich, D. B.; Mowat, J. H.; Patrick, J. B.; Broshard, R. W.; Meyer, W. E.; Williams, R. P.; Wolf, C. F.; Fulmor, W.; Pidacks, C.; Lancaster, J. E. The Structures of Mitomycins A, B and C and Porfiromycin-Part I. *J. Am. Chem. Soc.* **1962**, *84*, 3185-3187.
3. Webb, J. S.; Cosulich, D. B.; Mowat, J. H.; Patrick, J. B.; Broshcard, R. W.; Meyer, W. E.; Williams, R. P.; Wolf, C. F.; Fulmor, W.; Pidacks, C.; Lancaster, J. E. The Structures of Mitomycins A, B, and C and Porfiromycin – Part II. *J. Am. Chem. Soc.* **1962**, *84*, 3187-3188.
4. Remers, W. A. *Anticancer Agents from Natural Products*, 2nd ed.; CRC Press.
5. Kinoshita, S.; Uzu, K.; Nakano, K.; Shimizu, M.; Takahashi, T. Mitomycin Derivatives. 1. Preparation of Mitosane and Mitosene Compounds and Their Biological Activities. *J. Med. Chem.* **1971**, *14*, 103-109.
6. Hodges, J. C.; Remers, W. A. Synthesis and Antineoplastic Activity of Mitosene Analogues of the Mitomycins. *J. Med. Chem.* **1981**, *24*, 1184-1191.
7. Iyengar, B. S.; Remers, W. A.; Bradner, W. T. Preparation and Antitumor Activity of 7-Substituted 1,2-Aziridinomitosenes. *J. Med. Chem.* **1986**, *29*, 1864-1868.
8. Teng, S. P.; Woodson, S. A.; Crothers, D. M. DNA Sequence Specificity of Mitomycin Cross-Linking. *Biochemistry* **1989**, *28*, 3901-3907.
9. Li, V.-S.; Choi, D.; Tang, M.-S.; Kohn, H. Concerning *in Vitro* Mitomycin-DNA Alkylation. *J. Am. Chem. Soc.* **1996**, *118*, 3765-3766.
10. Vedejs, E.; Naidu, B. N.; Klapars, A.; Warner, D. L.; Li, V.-s.; Na, Y.; Kohn, H. Synthetic Enantiopure Aziridinomitosenes: Preparation, Reactivity, and DNA Alkylation Studies. *J. Am. Chem. Soc.* **2003**, *125*, 15796-15806.
11. Rink, S. M.; Warner, D. L.; Klapars, A.; Vedejs, E. Sequence-Specific DNA Interstrand Cross-Linking by an Aziridinomitosene in the *Absence* of Exogenous Reductant. *Biochemistry*, **2005**, *44*, 13981-13986.
12. Davis Jr., W.; Ronai, Z.; Tew, K. D. Cellular Thiols and Reactive Oxygen Species in Drug-Induced Apoptosis. *J. Pharmacol. Exp. Ther.* **2001**, *296*, 1-6.
13. Handa, K.; Sato, S. Generation of Free Radicals of Quinone Group-Containing Anti-Cancer Chemicals in NADPH-Microsome System as Evidence by Initiation of Sulfite Oxidation. *Gann* **1975**, *66*, 43-47.

14. Tomasz, M. H_2O_2 Generation During the Redox Cycle of Mitomycin C and DNA-bound Mitomycin C. *Chem.-Biol. Interact.* **1976**, *13*, 89-97.

15. Lown, J. W.; Sim, S.-K.; Chen, H.-H. Hydroxyl radical production by free and DNA-bound aminoquinone antibiotics and its role in DNA degradation. Electron spin resonance detection of hydroxyl radicals by spin trapping. *Can. J. Biochem.* **1978**, *56*, 1042-1047.

16. Bachur, N. R.; Gordon, S. L.; Gee, M. V. A General Mechanism for Microsomal Activation of Quinone Anticancer Agents to Free Radicals. *Cancer Res.* **1978**, *38*, 1745-1750.

17. Doroshow, J. H. Mitomycin C-Enhanced Superoxide and Hydrogen Peroxide Formation in Rat Heart. *J. Pharmacol. Exp. Ther.* **1981**, *218*, 206-211.

18. Komiyama, T.; Kikuchi, T.; Sugiura, Y. Generation of Hydroxyl Radical by Anticancer Quinone Drugs, Carbazilquinone, Mitomyin C, Aclacinomycin A and Adriamycin, in the Presence of NADPH-Cytochrome P-450 Reductase. *Biochem. Pharmacol.* **1982**, *31*, 3651-3656.

19. Wang, H.; Joseph, J. A. Quantifying Cellular Oxidative Stress by Dichlorofluorescein Assay Using Microplate Reader. *Free Radical Biol. Med.* **1999**, *27*, 612-616.

20. Pritsos, C. A.; Sartorelli, A. C. Generation of Reactive Oxygen Radicals through Bioactivation of Mitomycin Antibiotics. *Cancer Res.* **1986**, *46*, 3528-3532.

21. Collier, A. C.; Pritsos, K. L.; Pritsos, C. A. TCDD as a biological response modifier for Mitomycin C: Oxygen tension affects enzyme activation, reactive oxygen species and cell death. *Life Sciences*, **2006**, *78*, 1499-1507.

22. Nordberg, J.; Arnér, E. S. J. Reactive Oxygen Species, Antioxidants, and the Mammalian Thioredoxin System. *Free Radical Biol. Med.*, **2001**, *31*, 1287-1312.

23. Klaunig, J. E.; Kamendulis, L. M. The Role of Oxidative Stress in Carcinogenesis. *Annu. Rev. Pharmacol. Toxicol.* **2004**, *44*, 239-267.

24. abcam. ab113850 – JC1-Mitochondrial Membrane Potential Assay Kit. Version 1. Accessed April 26, 2013.

25. Nicholls, D. G. Mitochondrial function and dysfunction in the cell: its relevance to aging and aging-related disease. *Int. J. Biochem. Cell Biol.* **2002**, *34*, 1372-1381.

26. Salvioli, S.; Ardizzoni, A.; Franceschi, C.; Cossarizza, A. JC-1, but not DiOC6(3) or rhodamine 123, is a reliable fluorescent prove to assess $\Delta\Psi$ changes in intact cells: implications for studies on mitochondrial functionality during apoptosis. *FEBS Letters*, **1997**, *411*, 77-82.

27. Mancini, M.; Anderson, B. O.; Caldwell, E.; Sedghinasab, M.; Paty, P. B.; Hockenbery, D. M. Mitochondrial Proliferation and Paradoxical Membrane Depolarization during Terminal Differentiation and Apoptosis in a Human Colon Carcinoma Cell Line.

28. Gottlieb, R. A. Mitochondria: execution central. *FEBS Letters*, **2000**, *482*, 6-12.

29. Han, S.; Espinoza, L. A.; Liao, H.; Boulares, A. H.; Smulson, M. E. Protection by antioxidants against toxicity and apoptosis induced by the sulphur mustard analog 2-chloroethylethyl sulphide (CEES) in Jurkat T cells and normal human lymphocytes. *Br. J. Pharmacol.* **2004**, *141*, 795-802.

30. Edinger, A. L.; Thompson, C. B. Death by design: apoptosis, necrosis and autophagy. *Curr. Opin. Cell Biol.* **2004**, *16*, 663-669.

31. Pirnia, F.; Schneider, E.; Betticher, D. C.; Borner, M. M. Mitomycin C induces apoptosis and caspase-8 and -9 processing through a caspase-3 and Fas-independent pathway. *Cell Death Differ.* **2002**, *9*, 905-914.

32. Boamah, E. K.; Brekman, A.; Tomasz, M.; Myeku, N.; Figueiredo-Pereira, M.; Hunter, S.; Meyer, J.; Bhosle, R. C.; Bargonetti, J. DNA Adducts of Decarbamoyl Mitomycin C Effeciently Kill Cells without Wild-Type p53 Resulting from Proteasome-Mediated Degradation of Checkpoint Protein 1. *Chem. Res. Toxicol.* **2010**, *23*, 1151-1162.

33. Hu, W.; Kavanagh, J. J. Anticancer therapy targeting the apoptotic pathway. *Lancet Oncol.* **2003**, *4*, 721-729.

34. Chowdhury, I.; Tharakan, B.; Bhat, G. K. Caspases – An update. *Comp. Biochem. Physiol., Part B: Biochem. Mol. Biol.* **2008**, *151*, 10-27.

35. O'Brien, J.; Wilson, I.; Orton, T.; Pognan, F. Investigation of the Alamar Blue (resazurin) fluorescent dye for the assessment of mammalian cell cytotoxicity. *Eur. J. Biochem.* **2000**, *267*, 5421-5426.

36. Hamid, R.; Rotshteyn, Y.; Rabadi, L.; Parikh, R.; Bullock, R. Comparison of alamar blue and MTT assays for high through-put screening. *Toxicol. In Vitro* **2004**, *18*, 703-710.

37. Verweij, J.; Pinedo, H. M. Mitomycin C: mechanism of action, usefulness and limitations. *Anti-Cancer Drugs* **1990**, *1*, 5-13.

38. Shi, K.; Wang, D.; Cao, X.; Ge, Y. Endoplasmic Reticulum Stress Signaling Is Involved in Mitomycin C(MMC)-Induced Apoptosis in Human Fibroblasts via PERK Pathway. *PLoS One* [Online] **2013**, *8*, 1-12 http://www.plosone.org/article/info%3Adoi%2F10.1371%2Fjournal.pone.0059330 (Accessed May 31, 2014).

39. abcam. ab113851 – DCFDA Cellular ROS Detection Assay Kit. Version 1. Accessed April 26, 2013.

40. Paz, M. M.; Das, A.; Palom, Y.; He, Q.-Y.; Tomasz, M. Selective Activation of Mitomycin A by Thiols To Form DNA Cross-links and Monoadducts: Biochemical Basis for the Modulation of Mitomycin Cytotoxicity by the Quinone Redox Potential. *J. Med. Chem.* **2001**, *44*, 2834-2842.

41. Paz, M. M. Reductive Activation of Mitomycin C by Thiols: Kinetics, Mechanism, and Biological Implications. *Chem. Res. Toxicol.* **2009**, *22*, 1663-1668.

42. Wu, K.-Y.; Wang, H.-Z.; Hong, S.-J. Mechanism of mitomycin-induced apoptosis in cultured corneal endothelial cell. *Mol. Vision* **2008**, *14*, 1705-1712.

43. Park, I.-C.; Park, M.-J.; Hwang, C.-S.; Rhee, C.-H.; Whang, D.-Y.; Jang, J.-J.; Choe, T.-B.; Hong, S.-I.; Lee, S.-H. Mitomycin C induces apoptosis in a caspases-dependent and Fas/CD95-independent manner in human gastric adenocarcinoma cells. *Cancer Lett.* **2000**, *158*, 125-132.

44. Sasaki, M.; Okamura, M.; Ideo, A.; Shimada, J.; Suzuki, F.; Ishihara, M.; Kikuchi, H.; Kanda, Y.; Kunii, S.; Sakagami, H. Re-evaluation of Tumor-specific Cytotoxicity of Mitomycin C, Bleomycin and Peplomycin. *Anticancer Res.* **2006**, *26*, 3373-3380.

45. Boamah, E. K.; White, D. E.; Talbott, K. E.; Arva, N. C.; Berman, D.; Tomasz, M.; Bargonetti, J. Mitomycin-DNA Adducts Induce p53-Dependent and p53-Independent Cell Death Pathways. *ACS Chem. Biol.* **2007**, *2*¸ 399-407.

46. Schulze-Osthoff, K. *Apoptosis, Cytotoxicity and Cell Proliferation*, 4th ed.; Roche Diagnostics GmbH; Mannheim, 2008.

47. Rasband, W.S., ImageJ, U. S. National Institutes of Health, Bethesda, Maryland, USA, http://imagej.nih.gov/ij/, 1997-2014.

CHAPTER THREE: MODIFICATION OF CELLULAR DNA BY AZIRIDINOMITOSENES

The ability of two synthetic aziridinomitosenes (AZMs) to modify DNA in Jurkat and HeLa cells was evaluated using a Hoechst 33342 fluorescent assay and modified alkaline Single Cell Gel Electrophoresis (COMET) assay. The Hoechst 33342 assay showed that (1S, 2S)-6-methyl(methylaziridino)mitosene (Me/H-AZM**)** treatment increased cross-linkage 48 and 6 fold greater than mitomycin C (MC) in Jurkat and HeLa cells, respectively. In contrast, (1S, 2S)-6-desmethyl(methylaziridino)mitosene (H/H-AZM) only increased the cross-linkage of DNA in Jurkat cells 12.5 fold greater than MC. In HeLa cells, H/H-AZM sponsored DNA cross-links were approximately two fold lower than MC. The modified alkaline COMET assay allows for the evaluation of DNA modification of a drug through the reduced migration of treated DNA. H/H-AZM treated cells showed significantly less DNA migration in the modified alkaline COMET assay with tail extent moments of 0.7% and 59.6% of MC in Jurkat and HeLa cells, respectively. Me/H-AZM tail extent moments in Jurkat and HeLa cells were found to be 0.3% and 6.3% of MC treated cells, correspondingly. The results of this study indicate that AZMs are capable of modifying DNA in *in vitro* cellular systems, with Me/H-AZM showing the most potent activity and greatest alterations to DNA.

Introduction

Aziridinomitosenes (AZMs) are a class of compounds that are structurally similar to mitomycin chemotherapeutics. The first synthesis, characterization, and preliminary biological activity of AZMs were reported in 1964.[1] Further, they present as an intermediate in the DNA alkylating reductive activation cascade of mitomycins.[2] Structurally, AZMs differ from mitomycins by the placement of a double bond between carbons 9 and 9a in the AZM architecture, whereas this is a single bond in mitomycins (Figure 3.1).[3] The double bond promotes the benzylic-like stabilization of electrophilic carbons 1 and 10, increasing their susceptibility to nucleophilic groups, such as the amines in DNA, thus leading to DNA cross-linking.

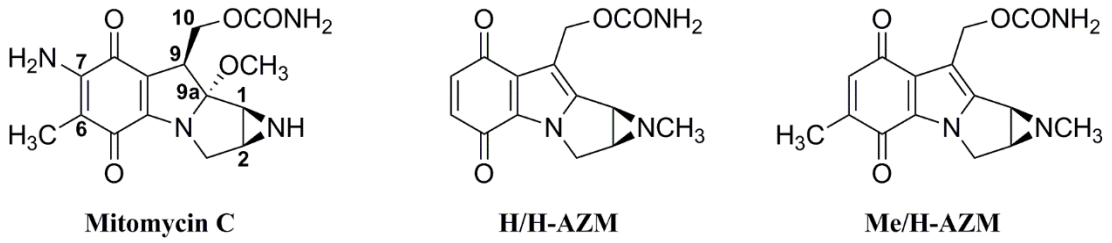

Mitomycin C **H/H-AZM** **Me/H-AZM**

Figure 3.1 Structures of mitomycin C and aziridinomitosenes. MC displays a partial carbon numbering scheme consistent with mitomycins and aziridinomitosenes. H/H-AZM = (1S, 2S)-6-desmethyl(methylaziridino)mitosene, Me/H-AZM = (1S, 2S)-6-methyl(methylaziridino)mitosene.

Of the mitomycins, MC has received the most attention and use as a chemotherapeutic agent. MC has been useful as a single agent or in combination therapy for a variety of different cancers including local bladder, head and neck, breast, and non-small cell lung cancers. Despite its widespread applications, MC use is limited due to severe side effects such as myelosuppression or haemolytic uremic syndrome.[4]

The biological activity of the mitomycins has been attributed to the formation of DNA-DNA interstrand cross-links (ICLs), a covalent modification between two

complimentary strands of DNA.[5,6] Prior to forming ICLs, MC must first undergo chemical or enzymatic reductive activation, rendering the drug electrophilic (Figure 3.2).[5,7-11] As such, MC induced cytotoxicity has shown preference towards hypoxic conditions, or those favoring its reductive activation.[11,12]

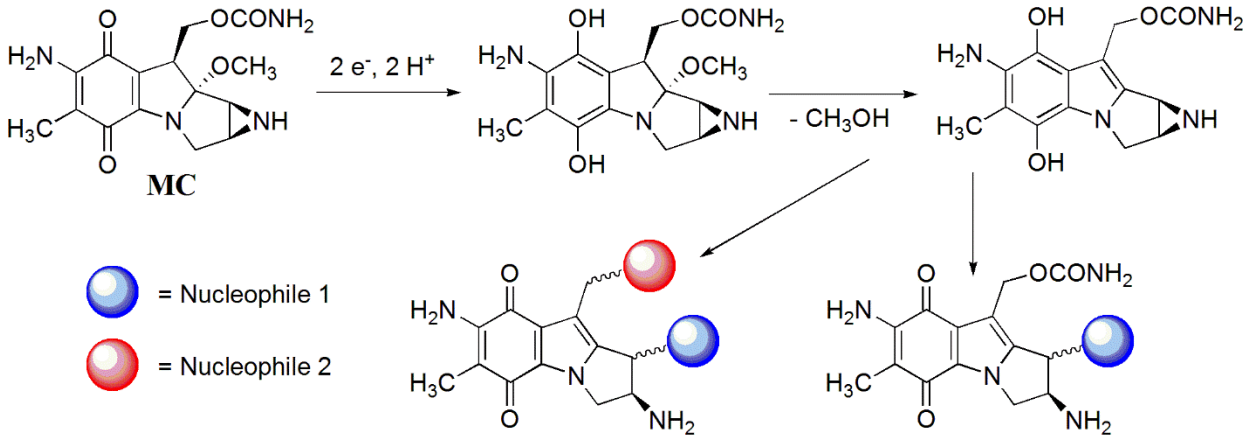

Figure 3.2 Reductive activation of MC. Reduction of MC leads to formation of a mono-alkylated (blue sphere only) or bis-alkylated (both blue and red spheres) compound.

The formation of ICLs with AZMs have been reported using purified synthetic or bacterial DNA in the presence and absence of reducing agents.[14-17] Similar to MC, AZMs exhibit a DNA sequence preference towards 5'-CpG-3' motifs.[14-17] The synthetic AZM, (1S, 2S)-6-desmethyl(methylaziridino)mitosene (H/H-AZM) has been shown to cross-link DNA with similar frequency and specificity as MC, with alkylation occurring preferentially at guanine residues.[13,16,17] Previous reports suggest that H/H-AZM may form both DNA-DNA and DNA-protein cross-links.[16] In contrast to MC, H/H-AZM was shown to cross-link synthetic DNA in the presence of oxygen, and did not require activation by exogenous reductants. Guanine nucleotides were confirmed as the nucleophilic species in the formation of H/H-AZM facilitated DNA ICLs.[17]

Prior investigations of DNA modification by AZMs were confined to demonstration of adduct formation with purified nucleic acids or oligonucleotides. The current study was initiated to establish that AZMs could cause modifications to DNA in eukaryotic cellular environments. We evaluated DNA modification induced by H/H-AZM and Me/H-AZM, in HeLa and Jurkat cell lines using a Hoechst 33342 fluorescent DNA cross-linking and modified alkaline COMET assays.[16,18,22,25,27,28]

Hoechst fluorescent DNA cross-linking studies have previously been conducted using Hoechst 33258 fluorescence with T7 coliphage DNA to study cross-linking agents, including reductively activated MC and its analogs.[18-20] The premise of this assay is that DNA cross-links will lead to increased retention of Hoechst fluorescence after a heat denaturation/rapid cooling process when compared to native DNA. Reductively activated MC and the decarbamoyl derivative (DMC) were found to cross-link T7 in a concentration dependent manner with this assay.[20] Here, we apply this method to DNA isolated from AZM treated human cancer cells in order to determine the relative amount of cross-linkage that occurred using the fluorescent DNA probe Hoechst 33342.

In its original development, the Single Cell Gel Electrophoresis (COMET) assay was used to identify DNA damaging agents and investigate the repair kinetics in cells.[21] Since then, variations to the COMET assay have been described that allow the detection of DNA cross-linking agents. These evaluations are based on the compound's ability to decrease the electrophoretic mobility of DNA when combined with DNA damaging agents.[22-24,26-28] In this study, as in previous studies with MC, we use a similar modified alkaline COMET assay to measure DNA cross-linkage in MC or AZM treated that were subsequently exposed to the DNA damaging agent hydrogen peroxide.[25]

Materials and Methods

Materials

MC was purchased from Cayman Chemical (Ann Arbor, MI). Hoechst 33342 was obtained from Invitrogen (Eugene, OR). A 10,000x SYBR Green solution was aquired from Molecular Probes (Eugene, OR). HyClone growth media (RPMI-1640 and Dulbecco's Modified Eagles Medium (DMEM)) and penicillin/streptomycin solution were obtained from Thermo Scientific (Waltham, MA). Fetal Bovine Serum (FBS) was purchased from Fisher Scientific (Hampton, NH). Blood and Cell Culture Mini Kit was obtained from Qiagen (Hilden, Germany). The CometAssay Kit was purchased from Trevigen (Gaithersburg, MD).

Cell Culture

Jurkat and HeLa cell lines were obtained as a generous gift from Dr. Denise Wingett, Dr. John Rasmussen, and Dr. Ken Cornell at Boise State University. Jurkat cells were cultured in RPMI-1640 supplemented with 10% FBS, penicillin (100 U/mL), and streptomycin (100 µg/mL). HeLa cells were cultured in DMEM with 10% FBS, penicillin (100 U/mg), and streptomycin (100 µg/mL). Cell lines were grown at 37 ºC in 5% CO_2 atmosphere.

Jurkat and HeLa Cell DNA Isolation

Jurkat and HeLa genomic and mitochondrial DNA were isolated together using the Qiagen DNA and Blood Mini Kit according to the manufacturer's recommendations for "Tissue" isolation. This protocol allows for the isolation of mitochondrial DNA as well as genomic DNA.[29] Prior to DNA isolation, Jurkat and HeLa cells were grown in

T25 flasks until approximately 90% confluent or ~5-6 x 10^6 cells were available. Cells were then treated with vehicle (1x PBS) or 10 μM MC, H/H-AZM, or Me/H-AZM for one hour. After one hour, cells were harvested, washed twice in 1x PBS, and the DNA isolated according to the manufacturer's directions for "Tissue" DNA isolation. DNA concentrations were determined using a SYBR green fluorescence assay.[30]

Hoechst 33342 DNA Cross-Linking Assay

The following protocol is an adaptation to cross-linking assay presented by Penketh, Shyam, and Sartorelli.[18] DNA utilized in these experiments were isolated as outlined above. Samples for the assay were prepared in the dark by combining isolated cellular DNA (3,750 ng) with 300 μL of 1.0 μg/mL Hoechst 33342 in nanopure H_2O. The total volume was brought to 3 mL with 0.5x TE buffer. Fluorescence (ex 360 nm/em 460 nm) of a 2 mL portion of each sample was then read on a Varian Cary Eclipse Fluorimeter (Palo Alto, CA). A solution of 2,700 μL 0.5x TE + 300 μL 1.0 μg/mL Hoechst 33342 was used as a blank. After the initial readings, the retention of fluorescence was measured after subjecting samples to a heat/chill process as follows: 5 minutes in a 96-98°C water bath, immediate chilling in an ice/water bath for 5 minutes, followed by incubation in a room temperature water bath for 5 minutes. The fluorescence measurement was repeated and the cross-linked fractions were determined using Equation 1:

$$\text{Cross-linked fraction} = \frac{\frac{E_A}{E_B} - \frac{C_A}{C_B}}{1 - \frac{C_A}{C_B}} \qquad \textit{Equation 1}$$

Where, C_A = fluorescence of control sample after heat/chill, C_B = fluorescence of control sample before heat chill, E_A = fluorescence of experimental sample after heat/chill, and E_B = fluorescence of experimental sample before heat/chill.

Data was analyzed in Microsoft Excel (Redmond, WA) and GraphPad Prism (www.graphpad.com). Values were presented as the mean ± SEM of two independent DNA isolations with measurements conducted in triplicate for each isolation.

Modified Alkaline COMET Assay

The alkaline COMET Assay was performed according to the manufacturer's protocol (Trevigen, Gaithersburg, MD) with minor modifications. Briefly, Jurkat and HeLa cells were harvested, washed once with complete media, and reconstituted to a final density of 1 x 10^5 cells/mL (Jurkat) or 2 x 10^5 cells/mL (HeLa) using complete media in sterile 1.5 mL micro-centrifuge tubes. Cells were then either treated with a final concentration of either 10 μM MC, H/H-AZM, Me/H-AZM, or 1x PBS for one hour at 37 °C in 5% CO_2 with agitation every 15 minutes. After one hour, the cells were harvested via centrifugation, washed once in 1x PBS (Ca^{2+} and Mg^{2+} free), then resuspended in 100 μM hydrogen peroxide in 1x PBS for 20 minutes (Jurkat) or 30 minutes (HeLa) at 4°C. Next, cells were harvested via centrifugation (5 min, 150 x g (Jurkat), 250 x g (HeLa)), washed twice, and suspended in 1 mL of 1x PBS (Ca^{2+} and Mg^{2+} free). A 50 μL portion of the cell suspension was then combined with 300-500 μL of 37 °C low melting point agarose. The resulting solution was mixed by inversion several times and a 50 μL portion spread evenly on the COMET slide. COMET slides were then allowed to solidify at 4 °C for 30 minutes in the dark, after which they were submerged in lysis solution overnight at 4 °C in the dark. The following day, the slides

were removed from the lysis solution and submerged in a freshly prepared alkaline DNA unwinding (pH >13) solution for 20 minutes at room temperature in the dark. Slides were then subjected to electrophoresis (20V, ~300 mA) in freshly made alkaline electrophoresis solution for 30 minutes at 4 °C. After electrophoresis, the slides were rinsed twice in fresh deionized water for 5 minutes, followed by a third washing in 70% ethanol for 5 minutes. Slides were then dried at 37 °C for 15 minutes, followed by staining with 1x SYBR Green solution in 1x TE (pH 8.0) for 30 minutes at room temperature in the dark. Slides were then briefly washed in deionized water and dried at 37°C for approximately 1-2 hours. COMETS were visualized and images captured using an AMG Evos fluorescent microscope (Mill Creek, WA) using the 10x objective and GFP filter. Analysis for tail extent moment was performed using the OpenComet plugin for ImageJ (NIH), and tail extent moments (mean ± SEM) plotted in GraphPad Prism 6.[31,32]

Results

Hoechst 33342 DNA Cross-Linking Assay

The thermal denaturation process followed by rapid cooling causes mismatching in the base pairing of DNA leading to a decrease in fluorescence. The Hoechst fluorophores preferentially bind to A-T rich regions through the minor groove of DNA.[33] When bound to double stranded DNA (dsDNA), Hoechst stains exhibit an increased fluorescence when compared to single stranded DNA (ssDNA). Covalent cross-links in the DNA act as anchor points, decreasing the mismatched base pairing during rapid

renaturation. Thus, DNA with more cross-linking will exhibit increased retention of fluorescence after the heat/chill process.[18]

The relative fraction of cross-linked DNA created by MC and AZMs were determined using isolated DNA from drug treated Jurkat and HeLa cells (Table 3.1, Figure 3.3). When Jurkat and HeLa cells were treated with 10 μM Me/H-AZM for one hour, there was a significant increase in the amount of cross-linked DNA when compared to MC and H/H-AZM treatment. The fraction of cross-linked fractions was calculated at 0.39 (± 0.01) and 0.29 (± 0.01) for Me/H-AZM treated Jurkat and HeLa cells, respectively. The cross-linking sponsored by Me/H-AZM treatment was 48 fold greater than MC treatment in Jurkat cells, and 6 fold higher than MC treatment in HeLa cells. Similarly, the fraction of cross-linked DNA was higher in H/H-AZM treated Jurkat cells than in HeLa cells. In the Jurkat cell line, H/H-AZM treatment increased the fraction of cross-linked DNA 12.5 fold greater than MC treatment. In contrast, MC treatment of HeLa cells resulted in a 1.7 fold increase in cross-linked DNA compared to H/H-AZM treatment. This suggests that Jurkat DNA is more susceptible to H/H-AZM sponsored cross-linkage.

Table 3.1 Hoechst 33342 Assay for Cross-Linked DNA. Data presented is the calculated mean fraction of cross-linked DNA (± SEM) for two experiments, n = 6.

	Fraction of Cross-Linked DNA	
Drug (10 μM)	**Jurkat cells**	**HeLa cells**
Mitomycin C	0.008 ± 0.003	0.045 ± 0.004
H/H-AZM	0.10 ± 0.03	0.026 ± 0.007
Me/H-AZM	0.39 ± 0.01	0.29 ± 0.01

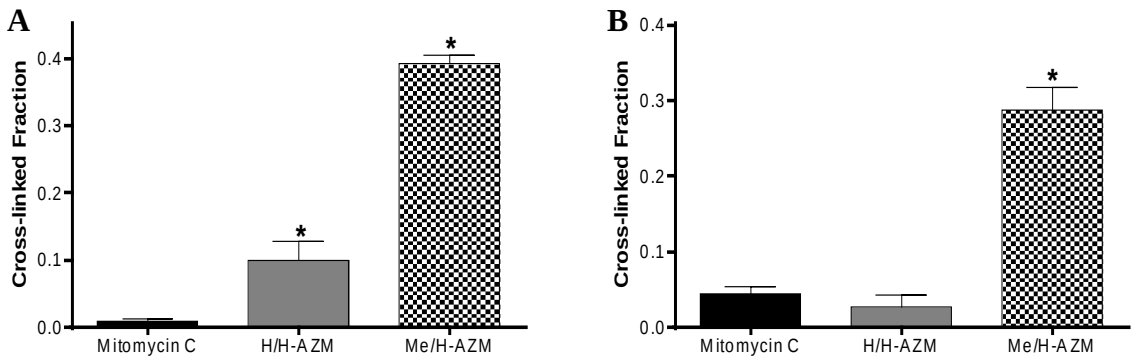

Figure 3.3 Hoechst 33342 DNA Cross-linking. A) Jurkat and B) HeLa cellular DNA was isolated after one hour treatment with either 10 µM mitomycin C, H/H-AZM, or Me/H-AZM. The fraction cross-linked of isolated DNA found in three drug treatments of A) Jurkat cells and B) HeLa cells was measured using Hoechst 33342 fluorescence. Data is presented as mean ± SEM of two experiments, n = 6, * denotes $p < 0.05$, by one-way ANOVA, when compared to Mitomycin C.

Modified Alkaline COMET Assay

The modified alkaline COMET assay provides the ability to investigate the extent of drug induced DNA cross-linking in individual cells. The alkaline COMET assay allows for visualization and quantification of DNA strand breakage, or damage and repair in single cells induced by DNA damaging agents.[19,26] The assay does not readily ascertain the ability to detect DNA alkylation events such as DNA interstrand, intrastrand, or DNA-protein cross-links.[26] Treatment with a genotoxic agent such as hydrogen peroxide induces DNA strand breaks that increases the electrophoretic mobility of DNA and results in the appearance of an elongated "tail" in the electropherogram. Agents that sponsor DNA cross-linking prior to hydrogen peroxide exposure ultimately hinder migration of DNA during electrophoresis by decreasing the amount of strand breaks that can occur.[22,23,25,26] This leads to a decreased tail length in the electropherogram when compared to cells only treated with hydrogen peroxide.[22,28] The "tail extent moment" is calculated by multiplying tail length by the measured amount of

DNA in the tail.[26] Previously, treatment of bladder cancer cell lines with MC was reported to cause DNA cross-linkage that resulted in decreased γ-radiation induced DNA strand breakage in the COMET assay. The DNA in the assay displayed decreased electrophoretic mobility, and a decreased "tail" in the electropherogram.[26] This type of modified alkaline COMET assay has also been used to demonstrated DNA cross-linkage by platinum containing chemotherapeutics, such as oxaliplatin and satraplatin.[28]

Results from our modified alkaline COMET assay indicate that treatment of Jurkat and HeLa cells with 10 μM drug treatment (MC, H/H-AZM, and Me/H-AZM) for one hour results in decreased electrophoretic mobility of the DNA (Figures 3.4 and 3.5). Jurkat cells treated with H/H-AZM and Me/H-AZM produced mean tail extent moments of 0.45 ± 0.07 and 0.17 ± 0.03, respectively. These tail extent moments were significantly reduced relative to MC treatment (Figure 3.4, panel F). Tail extent moments for MC were found to be 64.06 ± 7.04 in Jurkat cells, compared to that of 69.82 ± 5.50 for the 100 μM H_2O_2 treated control, indicating that MC was poorly effective at causing DNA cross-linkage under the aerobic conditions used in the assay. The AZMs appear to reduce tail extent moments at least 142 fold greater than MC in Jurkat cells.

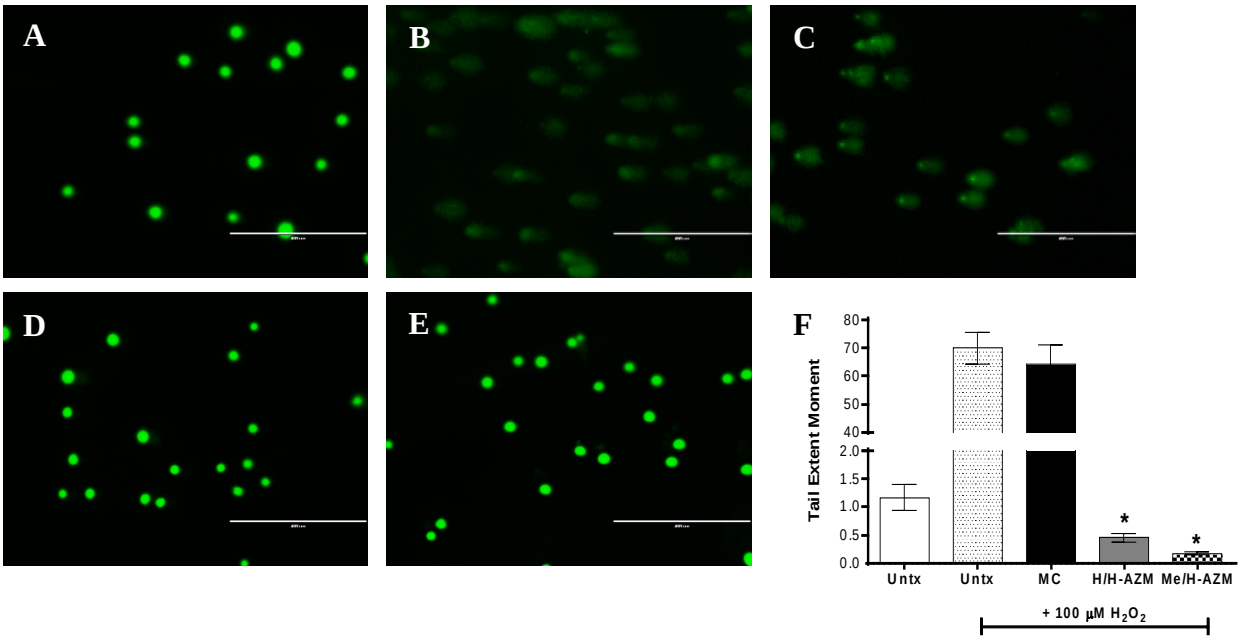

Figure 3.4 Modified Alkaline COMET assay of Jurkat cells. Jurkat cells were treated with either MC or AZM for one hour at 37ºC in 5% CO_2 atmosphere followed by exposure to 100 µM H_2O_2 for 20 minutes at 4 ºC to induce DNA strand breaks. Controls consisted of cells that received no drug (minimal DNA strand breaks), or received only H_2O_2 treatment (maximal DNA strand breaks). Panels show fluorescence micrographs of Jurkat cell electropherograms. Panel A) Vehicle w/o 100 µM H_2O_2; B) Vehicle + 100 µM H_2O_2; C) 10 µM mitomycin C + 100 µM H_2O_2; D) 10 µM H/H-AZM + 100 µM H_2O_2; E) 10 µM Me/H-AZM + 100 µM H_2O_2. Panel F) Plot of Jurkat cell tail extent moment. Tail extent moments are expressed as the mean ± SEM of two experiments (n > 50 cells per treatment). * Denotes p < 0.05 by one-way ANOVA, when compared to 100 µM H_2O_2 treated sample.

In contrast to Jurkat cells, HeLa cells appeared to be less sensitive to drug induced DNA cross-linkage (Figure 3.5). Tail extent moments in HeLa cells were the lowest in the Me/H-AZM treatment group (5.72 ± 0.73), followed by H/H-AZM treatment (53.77 ± 3.24). Both AZMs produced significant reductions in tail extent moments relative to the 100 µM H_2O_2 control. Me/H-AZM and H/H-AZM produced tail extent moments that were 15.8 and 1.7 fold lower, respectively, than MC treatment. Similar to the findings in Jurkat cells, MC treatment of HeLa cells produced tail extent moments (90.25 ± 4.17) that were insignificant when compared to the 100 µM H_2O_2 control (101.5 ± 4.6). Both

AZMs were able to significantly reduce the tail extent moments in HeLa cells to a greater extent than MC, with Me/H-AZM and H/H-AZM, 15.8 and 1.7 fold lower tail extent moments respectively (Figure 3.5).

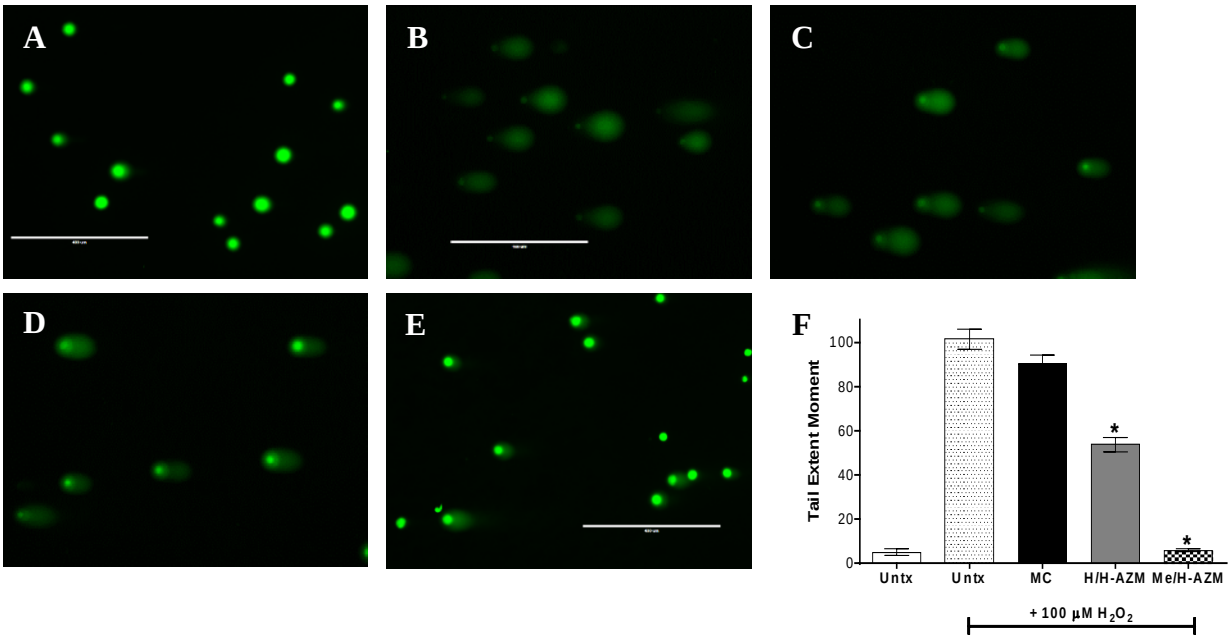

Figure 3.5 Modified Alkaline COMET assay of HeLa cells. HeLa cells were treated with either MC or AZM for one hour at 37ºC in 5% CO_2 atmosphere followed by exposure to 100 µM H_2O_2 for 30 minutes at 4 ºC to induce DNA strand breaks. Controls consisted of cells that received no drug (minimal DNA strand breaks), or received only H_2O_2 treatment (maximal DNA strand breaks). Panels show fluorescence micrographs of Jurkat cell electropherograms. Panel A) Vehicle w/o 100 µM H_2O_2; B) Vehicle + 100 µM H_2O_2; C) 10 µM mitomycin C + 100 µM H_2O_2; D) 10 µM H/H-AZM + 100 µM H_2O_2; E) 10 µM Me/H-AZM + 100 µM H_2O_2. Panel F) Plot of HeLa cell tail extent moment. Tail extent moments are expressed as the mean ± SEM of two experiments (n > 50 cells per treatment). * Denotes $p < 0.05$ by one-way ANOVA, when compared to 100 µM H_2O_2 treated sample.

Discussion and Conclusion

Results from the Hoechst 33342 cross-linking assay and modified alkaline COMET assay provide evidence that H/H-AZM and Me/H-AZM create DNA cross-links in Jurkat and HeLa cells after one hour of treatment in an aerobic environment. Me/H-AZM was more potent than H/H-AZM, particularly in Jurkat cells. MC treatment under

aerobic conditions resulted in insignificant DNA modification, which would be expected based on prior reports that demonstrated enhanced activation of MC for DNA cross-linking under anaerobic/reducing conditions.

The modified alkaline COMET assay provided insight into the occurrence of DNA alkylation events, although it does not distinguish between DNA-DNA or DNA-protein cross-links. However, the observed decreases in tail extent moments further support that cellular DNA is a target of AZM treatment that produces modifications (cross-linkages) that stabilize the structure and interfere with subsequent strand break formation. The differences in tail extent moments displayed by H/H-AZM in Jurkat and HeLa cells also provides evidence that Jurkat cell DNA is more vulnerable to DNA alkylation. These findings correspond well with the results of the Hoechst 33342 assay that showed that the fraction of cross-linked DNA was greater in AZM treated Jurkat cells compared to similar treatment of HeLa cells.

The Hoechst 33342 cross-linking assay utilizes DNA isolated from cells that have been treated with both RNAse-A and Proteinase K prior to purification. Since these enzymes act to cleave RNA and proteins and results in their removal from the system, the Hoechst assay should be more specific for the presence of DNA-DNA cross-links.[33,35] Interstrand cross-links are probably the most likely even since they would stabilize the double stranded DNA that would bind the Hoechst dye and result in retained fluorescence in the assay.[18,34] The formation of DNA-DNA cross-links by H/H-AZM is consistent with the formation of DNA-DNA interstrand cross-link formation reported by other investigators that examined AZM treatment of purified (cell free) radiolabelled DNA and UVrABC nuclease.[16,17]

AZM mediated DNA protein cross-links should still be considered as a relevant alkylation event, although not specifically measured here. While treatment with H/H-AZM and Me/H-AZM both produced similar reductions in tail extent moments in the COMET assay, the fraction of cross-linked DNA produced by Me/H-AZM treatment was approximately four fold greater as measured in the Hoechst assay, suggesting that other alkylation events are occurring besides DNA-DNA cross-links. The susceptibility to nucleophilic attack in H/H-AZM is present at four potential electrophilic locations at C1, C6/7, and C10. Prior reports by the Vedejs group demonstrated that H/H-AZM treatment resulted in the formation of high molecular weight DNA adducts that were tentatively attributed to AZM mediated DNA-protein cross-links.[16] Preliminary unpublished investigations within our laboratory have indicated that H/H-AZM is capable of forming DNA-protein cross-links with bovine serum albumin (BSA). The high intracellular concentration of protein, and particularly the presence of numerous DNA associated proteins (e.g., histones, etc.) that contain nucleophilic amine groups that could react with AZMs, suggest that the formation of a DNA-protein cross-link is highly probable. While additional work is required for the identification and subsequent characterization of AZM induced intracellular DNA-protein cross-links, the modified alkaline COMET assay could lend supplementary insight. While the alkaline method utilized in these experiments is reported to remove histones from DNA during the lysis process, this step occurs after AZM treatment, which leads us to postulate that DNA-protein cross-links (e.g., DNA-histone) may be retained in the assay. Further investigations should be directed towards measurement of the capability of AZMs to mediate DNA-protein cross-links and characterization of the alkylated adduct.

The increased DNA alkylation displayed by Me/H-AZM over H/H-AZM may be attributed to conservation of the methyl group at C6 that occurs throughout the A, B, and G-type mitomycins.[36] The methyl group is the sole structural difference between Me/H-AZM and H/H-AZM. Yet, this simple alteration results in a remarkable increase in cytotoxicity and DNA modification in two different cell lines. The methyl group may help to increase the lipophilicity of the aziridinomitosene that subsequently improves its cellular uptake and retention and increases its intracellular concentration. More likely, however, the presence of the inductive electron donation from the methyl group leads to increased stabilization of the electrophilic sites, resulting in a more stable DNA alkylating compound. Furthermore, the methyl group at C6 may sterically hinder nucleophile accessibility to the quinone ring, thus improving the half-life of the AZM by preventing non-productive reactions with other biomolecules outside the context of the DNA.

In conclusion, two synthetic AZMs produced within our lab were able to modify DNA in a cellular setting with similar or increased efficacy relative to MC, as indicated by Hoechst 33342 fluorescence and modified alkaline COMET assays. The addition of a methyl group at C6 in the AZM skeleton (Me/H-AZM) led to increased DNA cross-linking in both Jurkat and HeLa cell lines. Future experiments will be directed towards determining the DNA alkylating abilities of additional AZM analogs with chemical modification at the C6, C7, and C10 positions. Furthermore, additional studies to characterize and confirm DNA-AZM-protein cross-links and DNA-AZM-DNA cross-links from treated cells are being explored.

References

1. Patrick, J. B.; Williams, R. P.; Meyer, W. E.; Fulmor, W.; Cosulich, D. B.; Broshard, R. W.; Webb, J. S. Aziridinomitosenes: A New Class of Antibiotics Related to the Mitomycins. *J. Am. Chem. Soc.* **1964**, *86*, 1889-1890.
2. Kumar, G. S.; Lipman, R.; Cummings, J.; Tomasz, M. Mitomycin C-DNA Adducts Generated by DT-Diaphorase. Revised Mechanism of the Enzymatic Reductive Activation of Mitomycin C. *Biochemistry* **1997**, *36*, 14128-14136.
3. Remers, W. A. *Anticancer Agents from Natural Products*, 2nd ed.; CRC Press.
4. Bradner, W. T. Mitomycin C: a clinical update. *Cancer Treat. Rev.* **2001**, *27*, 35-50.
5. Iyer, V. N.; Szybalski, W. A Molecular Mechanism of Mitomycin Action: Linking of Complementary DNA Strands. *Proc. Natl. Acad. Sci. U.S.A.* **1963**, *50*, 355-362.
6. Bargonetti, J.; Champeil, E.; Tomasz, M. Differential Toxicity of DNA Adducts of Mitomycin C. *J. Nucleic Acids* [Online] **2010**, Article 698960.
7. Kumar, G. S.; Lipman, R.; Cummings, J.; Tomasz, M. Mitomycin C-DNA Adducts Generated by DT-Diaphorase. Revised Mechanism of the Enzymatic Reductive Activation of Mitomycin C. *Biochemistry* **1997**, *36*, 14128-14136.
8. Tomasz, M. Mitomycin C: small, fast and deadly (but very selective). *Chem. Biol.* **1995**, *2*, 575-579.
9. Danishefsky, S. J.; Schkeryantz, J. M. Chemical Explorations Driven by an Enchantment with Mitomycinoids – A Twenty Year Account. *Synlett* **1995**, 475-490.
10. Paz, M. M.; Pritsos, C. A. Chapter Seven. The Molecular Toxicology of Mitomycin C. *Adv. Mol. Toxicol.* **2012**, *6*, 243-299.
11. Fracasso, P. M.; Sartorelli, A. C. Cytotoxicity and DNA Lesions Produced by Mitomycin C and Porfiromycin in Hypoxic and Aerobic EMT6 and Chinese Hamster Ovary Cells. *Cancer Res.* **1986**, *46*, 3939-3944.
12. Keyes, S. R.; Loomis, R.; DiGiovanna, M. P.; Pritsos, C. A.; Rockwell, S.; Sartorelli, A. C. Cytotoxicity and DNA Crosslinks Produced by Mitomycin Analogs in Aerobic and Hypoxic EMT6 Cells. *Cancer Commun.* **1991**, *3*, 351-356.
13. Vedejs, E.; Klapars, A.; Naidu, B. N.; Piotrowski, D. W.; Tucci, F. C. Enantiocontrolled Synthesis of (1*S*,2*S*)-6-Desmethyl-(methylaziridino)mitosene. *J. Am. Chem. Soc.* **2000**, *122*, 5401-5402.
14. Teng, S. P.; Woodson, S. A.; Crothers, D. M. DNA Sequence Specificity of Mitomycin Cross-Linking. *Biochemistry* **1989**, *28*, 3901-3907.

15. Li, V.-S.; Choi, D.; Tang, M.-S.; Kohn, H. Concerning *in Vitro* Mitomycin-DNA Alkylation. *J. Am. Chem. Soc.* **1996**, *118*, 3765-3766.

16. Vedejs, E.; Naidu, B. N.; Klapars, A.; Warner, D. L.; Li, V.-s.; Na, Y.; Kohn, H. Synthetic Enantiopure Aziridinomitosenes: Preparation, Reactivity, and DNA Alkylation Studies. *J. Am. Chem. Soc.* **2003**, *125*, 15796-15806.

17. Rink, S. M.; Warner, D. L.; Klapars, A.; Vedejs, E. Sequence-Specific DNA Interstrand Cross-Linking by an Aziridinomitosene in the *Absence* of Exogenous Reductant. *Biochemistry*, **2005**, *44*, 13981-13986.

18. Penketh, P. G.; Shyam, K.; Sartorelli, A. C. Fluorometric Assay for the Determination of DNA-DNA Cross-Links Utilizing Hoechst 33258 at Neutral pH Values. *Anal. Biochem.* **1997**, *252*, 210-213.

19. Penketh, P. G.; Hodnick, W. F.; Belcourt, M. F.; Shyam, K.; Sherman, D. H.; Sartorelli, A. C. Inhibition of DNA Cross-linking by Mitomycin C by Peroxidase-mediated Oxidation of Mitomycin C Hydroquinone. *J. Biol. Chem.* **2001**, *276*, 34445-34452.

20. Palom, Y.; Kumar, G. S.; Tang, L.-Q.; Paz, M. M.; Musser, S. M.; Rockwell, S.; Tomasz, M. Relative Toxicities of DNA Cross-Links and Monoadducts: New Insights from Studies of Decarbamoyl Mitomycin C and Mitomycin C. *Chem. Res. Toxicol.* **2002**, *15*¸ 1398-1406.

21. Singh, N. P.; McCoy, M. T.; Tice, R. R.; Schneider, E. L. A Simple Technique for Quantitation of Low Levels of DNA Damage in Individual Cells. *Exp. Cell. Res.* **1988**, *175*, 184-191.

22. Pfuhler, S.; Wolf, H. U. Detection of DNA-Crosslinking Agents With the Alkaline Comet Assay. *Environ. Mol. Mutagen.* **1996**, *27*, 196-201.

23. Tice, R. R.; Yager, J. W.; Andrews, P.; Crecelius, E. Effect of hepatic methyl donor status on urinary excretion and DNA damage in B6C3F1 mice treated with sodium arsenite. *Mutat. Res.* **1997**, *386*, 315-334.

24. Merk, O.; Speit, G. Detection of Crosslinks With the Comet Assay in Relationship to Genotoxicity and Cytotoxicity. *Environ. Mol. Mutagen.* **1999**, *33*, 167-172.

25. Volpato, M.; Seargent, J.; Loadman, P. M.; Phillips, R. M. Formation of DNA interstrand cross-links as a marker of Mitomycin C bioreductive activation and chemosensitivity. *Eur. J. Cancer* **2005**, *41*, 1331-1338.

26. Tice, R. R.; Agurell, E.; Anderson, D.; Burlinson, B.; Hartmann, A.; Kobayashi, H.; Miyamae, Y.; Rojas, E.; Ryu, J.-C.; Sasaki, Y. F. Single Cell Gel/Comet Assay: Guidelines for In Vitro and In Vivo Genetic Toxicology Testing. *Environ. Mol. Mutagen.* **2000**, *35*, 206-221.

27. McKenna, D. J.; Gallus, M.; McKeown, S. R.; Downes, C. S.; McKelvey-Martin, V. J. Modification of the alkaline Comet Assay to allow simultaneous evaluation

of mitomycin C-induced DNA cross-link damage and repair of specific DNA sequences in RT4 cells. *DNA Repair* **2003**, *2*, 879-890.

28. Alotaibi, A.; Baumgartner, A.; Najafzadeh, M.; Cemeli, E.; Anderson, D. *In Vitro* Investigation of DNA Damage Induced by the DNA Cross-Linking Agents Oxaliplatin and Satraplatin in Lymphocytes of Colorectal Cancer Patients. *J. Cancer Ther.* **2012**, *3*, 78-89.
29. Boamah, E. K.; Brekman, A.; Tomasz, M.; Myeku, N.; Figueiredo-Pereira, M.; Hunter, S.; Meyer, J.; Bhosle, R. C.; Bargonetti, J. DNA Adducts of Decarbamoyl Mitomycin C Efficiently Kill Cells without Wild-Type p53 Resulting from Proteasome-Mediated Degradation of Checkpoint Protein 1. *Chem. Res. Toxicol.* **2010**, *23*, 1151-1162.
30. Santos, J. H.; Meyer, J. N.; Mandavilli, B. S.; Van Houten, B. Quantitative PCR-based measurement of nuclear and mitochondrial DNA damage and repair in mammalian, cells. *Methods Mol Biol.* **2006**, *314*, 183-199.
31. Rasband, W.S., ImageJ, U. S. National Institutes of Health, Bethesda, Maryland, USA, http://imagej.nih.gov/ij/, 1997-2014.
32. Gyori, B. M.; Venkatachalam, G.; Thiagarajan, P. S.; Hsu, D.; Clement, M.-V. OpenComet: An automated tool for comet assay image analysis. *Redox Biology* **2014**, *2*, 457-465.
33. Portugal, J.; Waring, M. J. Assignment of DNA binding sites for 4',6-diamidine-2-phenylindole and bisbenzimide (Hoechst 33258). A comparative footprinting study. *Biochim. Biophys. Acta, Gene Struct. Experssion* **1988**, *949*, 158-168.
34. Lown, J. W.; Begleiter, A.; Johnson, D.; Morgan, A. R.; Studies related to antitumor antibiotics. Part V. Reactions of mitomycin C with DNA examined by ethidium fluorescence assay. *Can. J. Biochem.* **1976**, *54*, 110-119.
35. Shoulkamy, M. I.; Nakano, T.; Ohshima, M.; Hirayama, R.; Uzawa, A.; Furusawa, Y.; Ide, H. Detection of DNA-protein crosslinks (DPCs) by novel direct fluorescence labeling methods: distinct stabilities of aldehyde and radiation-induced DPCs. *Nucleic Acids Res.* **2012**, *40*, e143.
36. Bass, P. D.; Gubler, D. A.; Judd, T. C.; Williams, R. M. Mitomycinoid Alkaloids: Mechanism of Action, Biosynthesis, Total Synthesis, and Synthetic Approaches. *Chem. Rev.* **2013**, *113*, 6816-6863.